MATHEMATICAL MODELING OF CSF DYNAMIC FORCE AND QUANTIFICATION OF CSF VELOCITY AT THE NARROWEST POINT OF AQUEDUCT OF SYLVIA BY CFD ANALYSIS

BY

AMILA HEMANTHA THALAKOTUNAGE

A THESIS SUBMITTED IN PARTIAL FULFILLMENT OF THE
REQUIREMENTS FOR THE DEGREE OF MASTER OF SCIENCE
(ENGINEERING AND TECHNOLOGY)
SIRINDHORN INTERNATIONAL INSTITUTE OF TECHNOLOGY
THAMMASAT UNIVERSITY
ACADEMIC YEAR 2015

MATHEMATICAL MODELING OF CSF DYNAMIC FORCE AND QUANTIFICATION OF CSF VELOCITY AT THE NARROWEST POINT OF AQUEDUCT OF SYLVIA BY CFD ANALYSIS

BY

AMILA HEMANTHA THALAKOTUNAGE

A THESIS SUBMITTED IN PARTIAL FULFILLMENT OF THE
REQUIREMENTS FOR THE DEGREE OF MASTER OF SCIENCE
(ENGINEERING AND TECHNOLOGY)
SIRINDHORN INTERNATIONAL INSTITUTE OF TECHNOLOGY
THAMMASAT UNIVERSITY
ACADEMIC YEAR 2015

MATHEMATICAL MODELING OF CSF DYNAMIC FORCE AND
QUANTIFICATION OF CSF VELOCITY AT THE NARROWEST POINT OF
AQUEDUCT OF SYLVIA BY CFD ANALYSIS

A Thesis Presented

By
AMILA HEMANTHA THALAKOTUNAGE

Submitted to
Sirindhorn International Institute of Technology
Thammasat University
In partial fulfillment of the requirements for the degree of
MASTER OF SCIENCE (ENGINEERING AND TECHNOLOGY)

Approved as to style and content by

Advisor and Chairperson of Thesis Committee _____
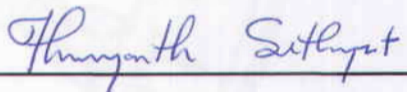
(Dr. Thunyaseth Sethaput)

Committee Member and
Chairperson of Examination Committee _____

(Asst.Prof.Dr. Anotai Suksangpanomrung)

Committee Member _____

(Dr. Sun Olapiriyakul)

Committee Member _____
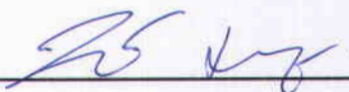
(Dr. Varalee Mingkwansook,M.D)

JUNE 2016

Acknowledgements

First and foremost I wish to extend my profound gratitude for all the peoples who contributed to made my higher study dream possible. Especially for Dr.Somnuk Tangtermsirikul (Professor) as a Director of Sirindhorn International Institute of Technology by accepting me as a Scholarship recipient. It is a great honor me to being as Student of SIIT-Thammasat University.

Also I wish to express my sincere appreciations to my advisor Dr. Thunyaseth Sethaput for believing and confidence placed on me by entrusting this research and thereafter for encouragement, guidance and excellent cooperation throughout the research.

Besides, I would like to thank my committee members, Dr. Sun Olapiriyakul, Asst.Prof.Dr. Anotai Suksangpanomrung and Dr. Varalee Mingkwansook who are always helped me in both academically and as elders since I am away from my country.

In addition, I am indebted thankful to Dr Varalee Mingkwansook-Thammasat Hospital and Assoc. Prof. Orasa Chawalparit-Mahidol University to giving me clinical data to continue my research. Theirs excitement and generosity conveyed me to complete this research possible. Without their supervision and constant help this research would not be good enough.

Last but not least, an honorable mention goes to my family and friends for their helps and supports for completing this research as well as being with me without making me alone.

Abstract

MATHEMATICAL MODELING OF CSF DYNAMIC FORCE AND
QUANTIFICATION OF CSF VELOCITY AT THE NARROWEST POINT OF
AQUEDUCT OF SYLVIA BY CFD ANALYSIS

by

AMILA HEMANTHA THALAKOTUNAGE

Bachelor of Science in Mechanical and Manufacturing Engineering,
University of Ruhuna-Sri Lanka, 2013

Master of Science (Engineering and Technology),
Sirindhorn International Institute of Technology,
Thammasat University-Thailand, 2015

Comprehensive knowledge in Cerebral spinal fluid dynamic behavior in brain would help to precisely explain about its pathological conditions such as Normal pressure hydrocephalus and after effects of traumatic brain injuries since root causes of these diseases are still controversies. Incognizance in circumstances of above disease leads to thousands of deaths per year from all over the earth. Especially, the Normal pressure hydrocephalus which is known as severe disorder condition mostly occur among elderly persons is not well defined. Typically, causes of the Normal pressure hydrocephalus is described as imbalance of Cerebral Spinal Fluid (CSF) formation and its absorption or obstruction in CSF motion. In near history scientist interpret root cause of Normal pressure hydrocephalus based on the bulk mass motion of CSF from the ventricles. But, later on researches shown that the bulk flow theory of CSF can no longer explain the cause of Normal pressure hydrocephalus and researches narrow to focus on pulsatile dynamic behavior of intracranial system and dynamics behavior of CSF through the cerebral aqueduct. Ventricular system of the brain can be basically divided in to four parts and cerebral aqueduct is the smallest part of ventricular system which acts as a linking passage between ventricles and

subarachnoid space of the spinal cord. Since cerebral aqueduct is the hub point of CSF distribution, it is easy to recognize any abnormalities of CSF formation and absorption by observing about the cerebral aqueduct. Development of mathematical model based on the behaviors of CSF motion through the cerebral aqueduct is the most reliable method. Magnetic Resonance Imaging can be used to examine the abnormalities in lateral ventricles and third ventricles by enlarging them. But, cerebral aqueduct was being less examined part because of its small dimensions. (MRI) and Computational Tomography (CT) observations are expensive and also due to the limited access of good health care system in third world country inhabitants.

CSF flow across the cerebral aqueduct is influenced by the several factors. Though choroid plexus continuously generate cerebral spinal fluids, its pulsatile motion which is synchronized with the systole and diastole interprets a correlation between CSF driving force and cardiac cycle. In this comprehensive study, author paid attention to the correlation of cardiac cycle and CSF pulsatile motion to develop a math model which can described CSF driving force by considering the arterial wall expansion and contraction. In order to develop a mathematical model, number of parameters has been considered and MRI data was highly helpful. Subsequently, author has been able to successfully define the CSF driving force. Math-model has been analytically and computationally validated by comparing the results with actual clinical data.

Developed math model was applied to predict the CSF velocity variation through the narrowest part of aqueduct in normal and normal pressure hydrocephalus patient. This has been done by CFD analysis, solid models which were used to analysis were developed by using MRI DICOM files of patients admitted to Thammasat hospital.

Author has noticed that, maximum velocity of CSF exerts in the narrowest point of aqueduct. Quantitatively, maximum velocity of CSF of NPH patient was considerably higher than the maximum velocity of CSF of normal patient.

After that, static pressure analysis for ventricular system has been done to examine the response of ventricular system with respect to the different intracranial pressure conditions correspond to different morphometric of aqueduct. Results

implied were, for NPH patients, lateral ventricles tend to expand to regulate the pressure while normal patients regulates ICP by expanding the volume of aqueduct.

Development of mathematical model to predict dynamic behavior of CSF through the cerebral aqueduct would be help to observe abnormalities of CSF motion and will help to identify hydrocephalus patients at their initial stage. Ultimately, this hypothesis might explore the understanding and direct the effective treatment procedure for the patient who suffers from disorder related to abnormalities of CSF motion.

Table of Contents

List of Tables

List of Figures

Chapter 1
Introduction

1.1 Statement of Problem

According to the statistics of recent studies, almost 700,000 matured Americans are subjected to Normal pressure hydrocephalus (NPH) while thousands of hundreds older peoples in Asia and Africa are living with NPH even without diagnosed and treated. The statistics implied that up to eighty percent of Normal pressure hydrocephalus patients are still not recognized though the early diagnosis and treatments are require to prevent from severe brain damages. Individual patients of 5.2 million from all over the world who are recognized as dementia, 10-15% are recognized as normal pressure hydrocephalus patients which need to undergo treatments.

Further statistics evolves that, US government allocates 184 million dollars annually for the Normal pressure hydrocephalus patients reported in United States, that amount worth to 25,000 USD per one patient (Hydrocephalus, 2014). Though that much of expenditures affordable for United States, many other countries in Asia and Africa struggle to overcome this problem not because of enough money. Therefore, proper methodology to recognize Normal pressure hydrocephalus at early stage is become a prerequisite circumstance. Unrecognizing Normal pressure hydrocephalus at its early stage will leads to severe brain tissue damage and high health care cost for adults including Youngers.

Normal pressure hydrocephalus is a disorder condition in ventricles causing the excess accumulation of cerebral spinal fluid inside the ventricle cavities. This excessive fluid accumulation can be caused due to the obstruction for the CSF motion, overproduction and abnormalities of CSF absorption in arachnoid villi. Further, malfunctioning of CSF draining process increases the intracranial pressure. These build up pressure affects to the brain tissues and interfere to the healthy brain functions. The place that can be make the most obstruction is the aqueduct of Sylvia which is the linking passage of third ventricle to fourth ventricle. With its small

dimension and morphometric shapes, aqueduct is the most critical place which effects to the CSF motion.

Normal pressure hydrocephalus is a common disorder among the elderly peoples of age above 55 years old. But, there are some possibilities to occur in young stages as well. Early treatments can lead to full recovery for NPH. Since NPH is a subcategory of hydrocephalus and non-treatments could subsequently lead to hydrocephalus, it is better to start this literature review from the perspectives related to hydrocephalus and then to normal pressure hydrocephalus.

World Health Organization's statistics shows that one birth in every 2,000 affected by hydrocephalus and it is one of the most critical fatal condition in the world after the stroke and cancers. The term of hydrocephalus is conjunction by two Greek words of "Hydro" and "Cephalous" meanings with water and head. Even though name implies as water accumulation in head, it is Cerebral Spinal Fluid (CSF). CSF is a colorless fluid with the consistence of blood plasma and surrounds the brain, spinal cord and Sub arachnoid spaces (SAS) (Linninger, et al., 2007).

Root causes of Hydrocephalus are not precisely identified yet and still it is a controversy. It may results from inherited genetic abnormalities, neuromuscular disorders, intraventricular hemorrhage, diseases such as meningitis, tumors, traumatic head injury (mass lesion) or subarachnoid hemorrhage.

Prognosis of this phenomenon can interpreted as the imbalance of cerebral spinal fluid formation and absorption resulting with excessive accumulation of cerebral spinal fluid in ventricles. It leads to get inflated the ventricles and manipulate to increase the intracranial pressure. This pressure increment increases the stresses on brain tissues and cause to physiological abnormality of head. Further, disorder of CSF circulation from the ventricles to cisterns creates malfunction of,

- Compensation process for changes in intracranial blood volume
- Nutrient delivery to the brain and embarrassing the drainage process

To cure this disease, extensive understanding of diagnosis methods are important. Diagnosed of Hydrocephalus is being done by clinical neurological evaluation and based on the symptoms of patient. Computer Tomography (CT),

Magnetic Resonance Image (MRI), Ultrasonography and Pressure monitoring methods are the most common clinical evaluation methods used to diagnosis of hydrocephalus.

Among these, first three methods used electromagnetic waves to generate the cross sectional images of brain and evaluate the abnormalities.

Pressure monitoring are the physical surgery methods and presently conducted in two ways as Lumbar puncture (spinal tap) and intracranial pressure monitoring method. Consecutively both two methods investigate abnormal pressure patterns at subarachnoid spaces in spinal cord and ventricles. Lumbar puncture technique is used to insert a needle in to the SAS at spinal cord and intracranial pressure monitoring method is used to insert a catheter in to the lateral ventricles. Figure 1.1 (a) (Puncture, n.d.) and (b) (Method, n.d.) shows lumbar puncture and ICP monitoring methods respectively.
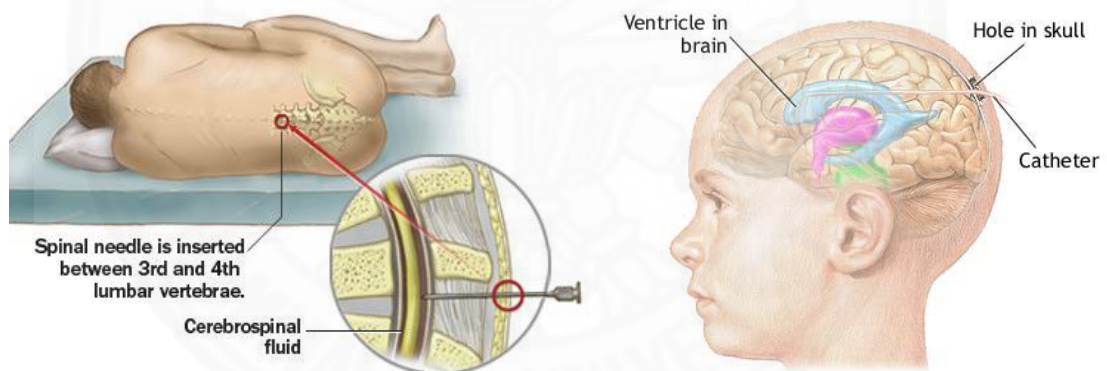
Figure 1.1. (a) Lumbar puncture (b) ICP Monitoring Method

None of aforementioned methods are pre prediction of disease and each and every method are used to confirmed the method of treatments, complementary methods for pre prediction of this disease by measuring abnormal pressure patterns and dynamic behavior of CSF is necessity.

While hydrocephalus mainly categorized in to two types as non-obstructive and obstructive hydrocephalus, each category also implies sub categories of hydrocephalus depends on the dementias and incontinences. Normal pressure

3

hydrocephalus is a significant subcategory of hydrocephalus among them. But for all entities of hydrocephalus, early diagnosis and treatments are inevitable to prevent long term disorder condition.

Normal pressure hydrocephalus primarily interpreted by Hakim and Adams in 1965 as, NPH pertain to a clinical circumstance including the triad of gait disturbance, dementia, and incontinence (Hakim & Adams, The special clinical problem of symptomatic hydrocephalus with normal cerebrospinal fluid pressure. Observations on cerebrospinal fluid hydrodynamics, 1965). Although NPH is an occasionally found disorder condition, early diagnosis is important since it is a treatable circumstance at the beginning. Radiologic inspection by magnetic resonance images (MRI- T2-weighted) of the brain is a better way to diagnosed NPH subjectively. Figure 1.2 shows brain MRI images of NPH patient which were reported in Thammasat hospital.
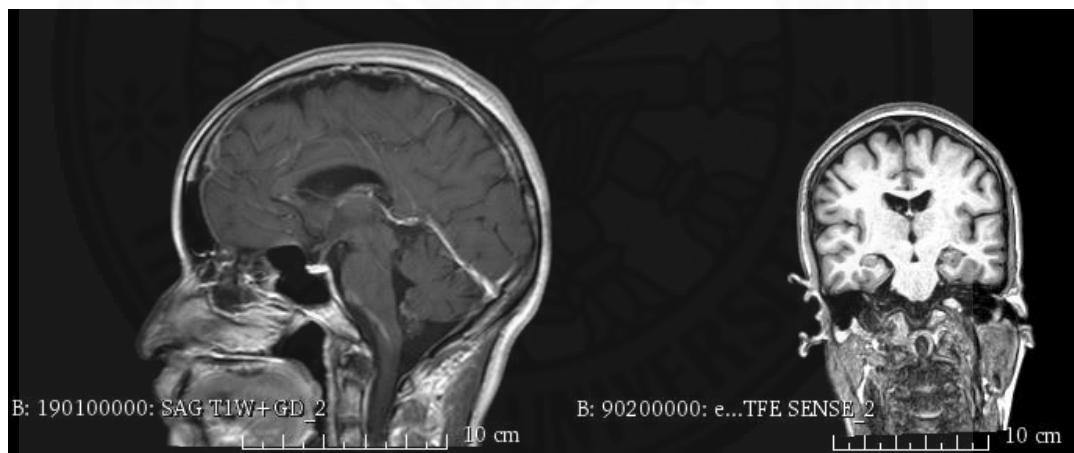
Figure 1.2. MRI of NPH patient reported in Thammasat Hospital

On imaging of MRI or CT, abnormalities of the lateral and third ventricles can be examine by enlarging them. But, it is not reliable due to the presence of very small parts (but having high impact) like aqueduct which is not easy to examine. Although not all NPH subjects does not show lateral and third ventricle abnormality, Normal pressure hydrocephalus (NPH) remains a controversial entity with often ambiguous imaging findings.

Our ultimate goal was to develop a mathematical model to predict the velocity pattern and dynamical behavior of Cerebral Spinal Fluid through the cerebral aqueduct and validate the results by using MRI data as well as by doing computational simulation. It would be help to identified Hydrocephalus patients at the pre stage of disease.

1.2 Purpose of study

The prognosis for individuals diagnosed with Normal pressure hydrocephalus is difficult to predict since portent of associated disorders, timeliness of diagnosis of Normal pressure hydrocephalus is indistinct yet. Although scientists have not confirmly identified the root causes of Normal pressure ydrocephalus, some remedial methods has been introduced. The most often treatment method is Shunt system and treated by surgically inserting a flexible plastic tube from ventricles to another area of the body (usually for stomach). Tube act as passage and allows to divert accumulated CSF from ventricles to where it can be absorbed as part of the normal circulatory process (National Institutes of Health, n.d.).

A shunt system consists of the shunt, a catheter and valve. One end of the catheter is placed within a ventricle inside the brain or in the Sub arachnoid spaces. The other end of the catheter is commonly placed within the abdominal cavity, but may also be placed at other sites in the body such as a chamber of the heart or areas around the lung where the CSF can drain and be absorbed. A valve located along the catheter maintains one way flow and regulates the rate of CSF flow (National Institutes of Health, n.d.).

Installing a shunt system is successful, but the problem encountered with it is required continual sustentation and medical supervision afterwards due to their propension for failure throughout the patient's life. Even with continuous monitoring, most shunts will fail occasionally and requiring immediate intensive care treatment to avoid death (Boston Children's Hospital, n.d.). In response, we wanted to develop a mathematical model to predict the dynamical behavior and the pressure variation of the CSF through the cerebral aqueduct to do continuous monitoring for patients. Not only for patients who already receiving treatments, Math model will manipulate to

predict the patients at their pre stage of disease and also it will help to decide the appropriate treatment method for doctors.

While the success of treatment with shunts varies from person to person, some people recover almost completely after treatment and have a good quality of life. Early diagnosis and treatment improves the chance of a good recovery.

Throughout this study, purposes were to define a math model which can interpret the governing force of cerebral spinal fluid and to develop a method to detect Normal pressure hydrocephalus at its early stage. Further, respond of ventricular tissues correspond to different intracranial pressure conditions was a purpose since it would help to develop relationship between Normal pressure hydrocephalus and intracranial pressure.

1.3 Significance of study

At the presence, most of the developed countries has been able to reduce the death rate of the Normal pressure hydrocephalus patients although they were unable to control the agent of disease and number of patients affected by each year. With the help of latest technology as MRI, CT Scanning for the prognosis and post-surgery monitoring, treatment methods as Shunting and endoscopic third ventriculostomy fit in to increase the life expectance of Normal pressure hydrocephalus patients in developed countries. But, either above prognosis or diagnosis methods are not feasible to the third world countries.

Majority of the inhabitants in third world countries are live below the poverty line and don not have access to the quality health. With having very low value of per capita income none of above prognosis or treatment methods are possible. World Health Organizations (WHO) statistics shows that significance number of Hydrocephalus patients reports on sub-Saharan Africa among the other third world countries. Availability of Neurosurgeon is one for 10 million peoples and there are almost a quarter million infant cases of hydrocephalus in Africa every year. Based on surgeon availability that would mean each neurosurgeon would have to treat a couple thousand cases annually (Thunyaseth, 2013).

The brain and spinal cord are surrounded by cerebrospinal fluid that is produced in the brain ventricles.

Fluid

Normal brain

In NPH cases, there is too much fluid because the brain can't drain the liquid.

Excess fluid

NPH brain

The ventricles enlarge to accommodate the extra fluid and put pressure on different parts of the brain, causing a number of symptoms.

Skull incision

Ventricle

Catheter

Excess fluid

Valve

Tubing runs under the scalp and the skin to the abdomen

The treatment for NPH patients involves the placement of an implantable shunt to drain fluid from the brain.

A one-way valve in the catheter allows the excess fluid to drain into the abdomen where it is reabsorbed.

Figure 1.3. Normal pressure hydrocephalus patient with shunt treatment (Normal Pressure Hydrocephalus, 2013)

Figure 1.3. Shows Normal pressure hydrocephalus patient with shunt treatment. Figure illustrates some abnormalities occurs when NPH growth and physiological changes in ventricular system.

Therefore Reliable and economically viable diagnosis method is necessity instead of MRI and CT Scanning. Throughout of this study, required clinical data and information were taken from Normal pressure hydrocephalus patient and all the simulations done based the particular patients' data. Normal pressure hydrocephalus eventually can grows up to fully hydrocephalus level. Hence, mathematical model to predict CSF abnormalities associated with ventricle system would be able to predict the Hydrocephalus at its initial stage. Requirements of Specialists can be reduced and patients can be evaluated by medical doctor after giving him a special training. If patient is in the initial stage of Hydrocephalus can be directed to the specialist. From this hypothesis, author implemented a Normal pressure hydrocephalus diagnosis method and hope it would be consolation for a mankind.

Chapter 2
Literature Review

Normal pressure hydrocephalus had been first identified and interpreted by S. Hakim and R.D Adams in 1965 (Hakim & Adams, The special clinical problem of symptomatic hydrocephalus with normal cerebrospinal fluid pressure. Observations on cerebrospinal fluid hydrodynamics, 1965). They had examined three patients with paradoxical condition of CSF motion which was a similar symptom of hydrocephalus, but with normal regular cerebrospinal fluid pressure. Traumatic encephalopathy or presenile or senile dementia which can be stated as occult hydrocephalic were their main diagnosed. Since this disorder conditioned implied as normal cerebrospinal pressure at the beginning, Hakim et.al had named it as Normal pressure hydrocephalus. The most important physical examination were, expansile force of the lateral ventricles were not similar to intraventricular pressure. But they did not certainly identified the cause of the normal pressure hydrocephalus and disease was considered as idiopathic condition. Further, congenital hydrocephalus conditions such as communicating hydrocephalus also they considered as Normal pressure hydrocephalus.

Thereafter, number of researches have been conducted by several researchers and W.G Bradley's (Bradley Jr, 2015) research is important among them. His findings were, to diagnose the Normal pressure hydrocephalus, enlarged ventricles to be detected by MRI and clinical triad are prerequisite. Gait disturbances has been identified as prominent symptom and dementia and urinary incontinence were the lasts. But these methods does not help to detect Normal pressure hydrocephalus at early stage. Because, according to W.G Bradley's clinical observations, some patients were only had dementia and it were difficult to identify the NPH. Therefore, MR imaging has been used as first diagnosis test for elderly patients to check ventricular dilation. Further, he had noticed a hyperdynamic CSF motion which similar to flow pattern of arterial blood. According to his MRI observations, hyperdynamic cerebral spinal fluid flow has been noted through the aqueduct when ventricular enlargement occurred. Patients with normal pressure hydrocephalus have also been found to have larger intracranial volumes than sex-

matched controls, suggesting that they may have had benign external hydrocephalus as infants. This were caused due to the decline of CSF reabsorption capacity by the arachnoid villi. With that, those patients showed a tendency to acquire parallel pathway foe cerebrospinal fluid drain from ventricles through extracellular apace. These circumstance ends when infant reached to adult age by showing two characteristic idiopathic normal pressure hydrocephalus conditions. Since normal pressure hydrocephalus initially can be started as hydrocephalus in infantry level, it is better to start literature review from the hydrocephalus and then to NPH.

Hydrocephalus comprises a miscellaneous group of disorders of CSF dynamics leading to an excessive accumulation of CSF within the brain, resulting in ventricular dilation and increased ICP (Intracranial Pressure). Simply it can be explain as imbalance of cerebral spinal fluid formation and absorption. Monro Kellie Doctoring theory is most conspicuous hypothesis which precisely explained the context of CSF volume, Brain volume, Arterial blood volume in skull and volume of Mass lesion for hydrocephalus phenomena. This method has greatly contributed to clinical research in the field of intracranial hypertension.

Even though Monro Kellie hypothesis explained the mechanism of how hydrocephalus happens the root causes for this pathogen is still controversies. Hence, the lack of appropriate diagnosis and remedies often undergo. Hydrocephalus was clinically studied for almost a century but the cause and understanding of this disorder were still incertitude. As a result of this, number of research has been done and is being doing yet. However, the modern clinical observation of MRI (Magnetic Resonance Interference) and CT Scanning (Computerized Tomography) data and experiments, new attention of hydrocephalus was focused on the pulsation of intracranial dynamics to explain that phenomena.

M. Egnor et al. (Egnor, Zheng, Rosiello, Gutman, & Davis, 2002) bring forward that Normal pressure hydrocephalus was caused by abnormality of intracranial pulsations which is caused by obstruction of the absorption of CSF at the arachnoid villi. Further they interpret CSF motion is Pulsatile and during the systole and diastole CSF associated with cranium and spinal shows the reciprocal motion across the Craniocervical junction. They have developed a model of intracranial pulsations based on the analogy between the pulsatile motion of electrons in an

electrical circuit and the pulsatile motion of blood and CSF in the cranium. Increased impedance to the flow of CSF pulsations in the subarachnoid space redistributes the flow of pulsations into the ventricular CSF and into the capillary and venous circulation. The salient features of Normal pressure hydrocephalus, such as ventricular dilation, intracranial pressure waves, narrowing of the CSF-venous pressure gradient, diminished cerebral blood flow, elevated resistive index and malabsorption of CSF, emerge naturally from the model. To validate their results clinical flow sensitive MRI data has been used and noticed that bulk flow of CSF with each cardiac cycle and most rapid bulk flow was in the spinal aqueduct. Hence subarachnoid CSF motion implies as pulsatile. Figure 2.1 illustrates the CSF pathway of human brain.
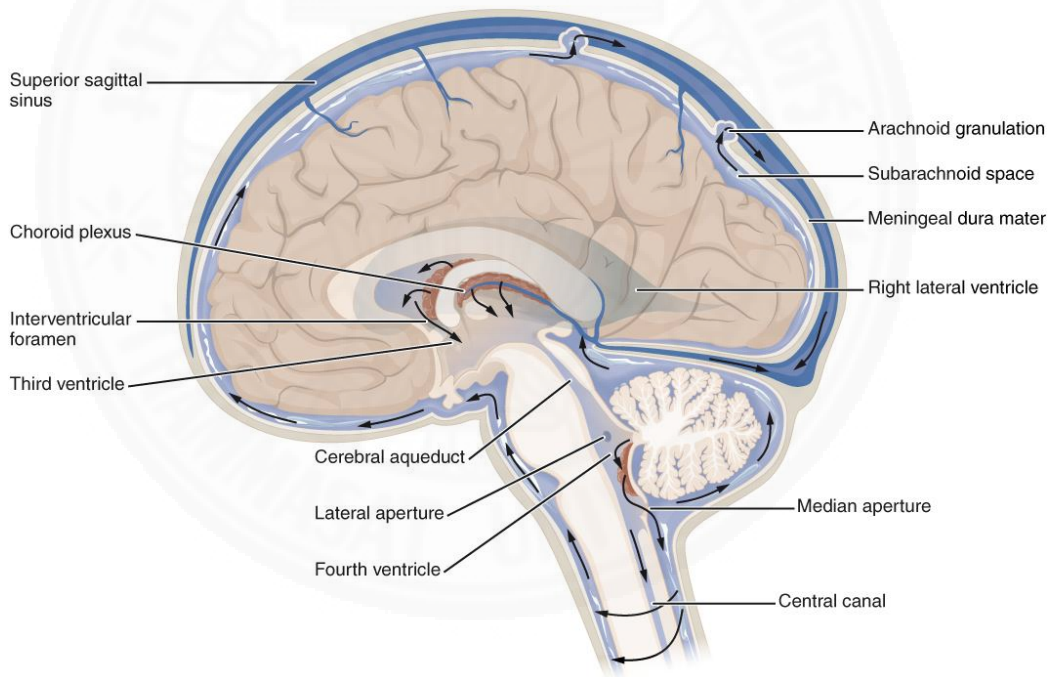
Figure 2.1. Cerebral Spinal Fluid circulation pathway in brain (CSF) (Pathway, n.d.)

But, their hypotheses does not contribute to predict dynamic behavior of the CSF bulk flow and pattern of the pulsations since they developed a model of intracranial pulsations based on the analogy between the pulsatile motion of electrons in an electrical circuit and the pulsatile motion of blood and CSF in the cranium. And

also diagnosis process for individual patient based on the symptoms is difficult by aforementioned method because of they used same circuit for an every examine.

Further, Andreas A. Linninger et al. (Linninger, et al., 2005) developed an extensive mathematical model for intracranial dynamics based on the first law of fluid mechanics. CSF oscillatory flow pattern and timing of the CSF motion with respect to the cardiac pulsation has been noted from MRI images. According to their mathematical model fluid motion obeys continuity and the Navier Stokes equations. The dynamics of parenchyma stresses, strains and displacements law of elastodynamics. Methodology was CSF oscillatory flow results from cardiac pulsations, pattern and timing of CSF motion has been studied extensively with MRI techniques. This hypothesis is supported by careful measurements of brain motion using CINE phase contrast. After combined gated MR with automated edge detection algorithms, observed a 10% - 20% variation in size of the lateral ventricles during the normal cardiac cycle. These measurements were not consistent with the brain motion hypothesis according to which arterial pulsation should diminish the ventricular size in the systole. But they did not count the non-Newtonian effect of cerebral blood and CSF. Since the CSF is non-Newtonian fluid, and viscosity depend on the amount of applied stress, it is an important factor to consider in simulations. So it shows different viscosities at different shear stresses. To take a distinct result several other rheological properties of CSF such as Oscillatory shears, stress and strain rate tensors under different flow conditions should be considered. The important similarities of those two researches were the perception of the pattern and motion of the CSF as oscillatory with respect to the cardiac cycle.

Figure 2.2 illustrates the pulsatile motion of CSF throughout the ventricular system.
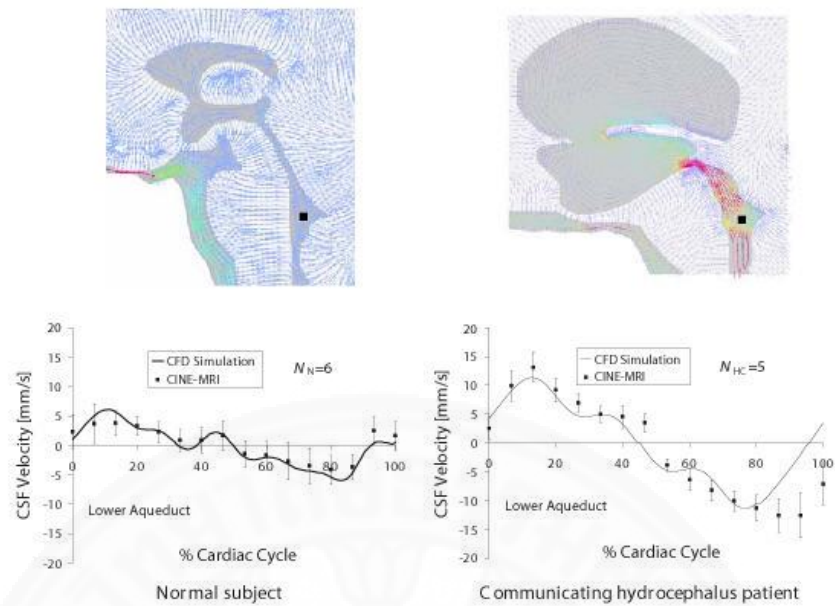
Figure 2.2. CSF Pulsatile motion with respect to the cardiac cycle (Sweetman, Xenos, Zitella, & Linninger, 2011)

    With the development of computer simulations researchers tended to the 3D modeling and simulations in the field of intracranial hypertension and hydrocephalus investigations. Brian Sweetman et al. (Sweetman, Xenos, Zitella, & Linninger, 2011) research is substantially important in this trend. They designed three-dimensional model of the human brain with ventricles as shown in Figure 2.3, Subarachnoid spaces (SAS) and other particular components associated with the human brain based on the patient specific geometries were reconstructed from magnetic resonance images. Image reconstructed model includes the entire cranial subarachnoid space as well as the entire ventricular system and used to predict the CSF flow field and intracranial pressures resulting from brain tissue displacement. Cine phase-contrast magnetic resonance imaging (CINE-MRI) was used to measure cranial CSF velocities in a normal subject and a patient diagnosed with Normal pressure hydrocephalus. Additional measurements included change in lateral ventricle size, CSF flow rate in the third ventricle and at the junction of the aqueduct and fourth ventricle, and the blood flow rate in the basilar artery. T2-weighted MR images of the cranium were manually segmented using image reconstruction software. The manual segmentation process resulted in patient specific, three dimensional triangulated surface meshes of a normal subject and a patient with communicating hydrocephalus.

12
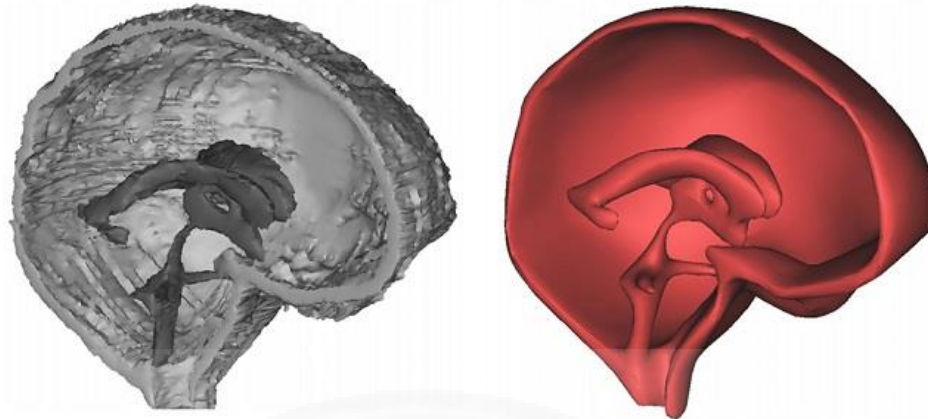
Figure 2.3. Manual Segmentation of the CSF filled spaces of the cranium resulted in the initially crude surface shown on the left. Advanced filtering techniques such as surface smoothing and triangle reduction resulted in the improved, more realistic surface displayed on the left (Sweetman, Xenos, Zitella, & Linninger, 2011)

After improving the reconstructed brain and ventricular surfaces, the surface meshes were imported into ADINA-FSI 8.6. In ADINA-FSI the meshes were discretized using Delaunay triangulation for the inner domain and the advancing front algorithm for the domain boundary. The mathematical models adopt physiologically relevant boundary conditions accounting for CSF production and pulsatility. The total CSF production of adult humans, approximately 0.5 ml/min and CSF was treated as a Newtonian fluid with viscosity and density similar to water. Assuming fluid incompressibility, continuity for CSF flow in the ventricles is written as Pulsating cerebral blood flow drives pulsatile CSF flow within the central nervous system (CNS). The process is driven by blood supply to the brain causing compliant arteries and arterioles to expand. Vascular expansion causes brain tissue stresses and displacements. In our model, tissue displacement compresses the lateral ventricles, forcing CSF into the subarachnoid space. Because the cranial volume remains constant, the total vascular expansion is matched by the sum of the CSF stroke volume expelled into the distensible spinal canal and the blood, which leaves the cranium through the venous sinuses. As the cerebral vasculature returns to its diastolic resting lumen, CSF expelled during cardiac systole flows back from the spinal canal to the cranial subarachnoid space. Then their simulated results ware validated by comparing the Cine phase-contrast MRI measurements. The model was enabled to

predict the complex CSF flow patterns and pressures in the ventricular system and subarachnoid space of a normal subject.
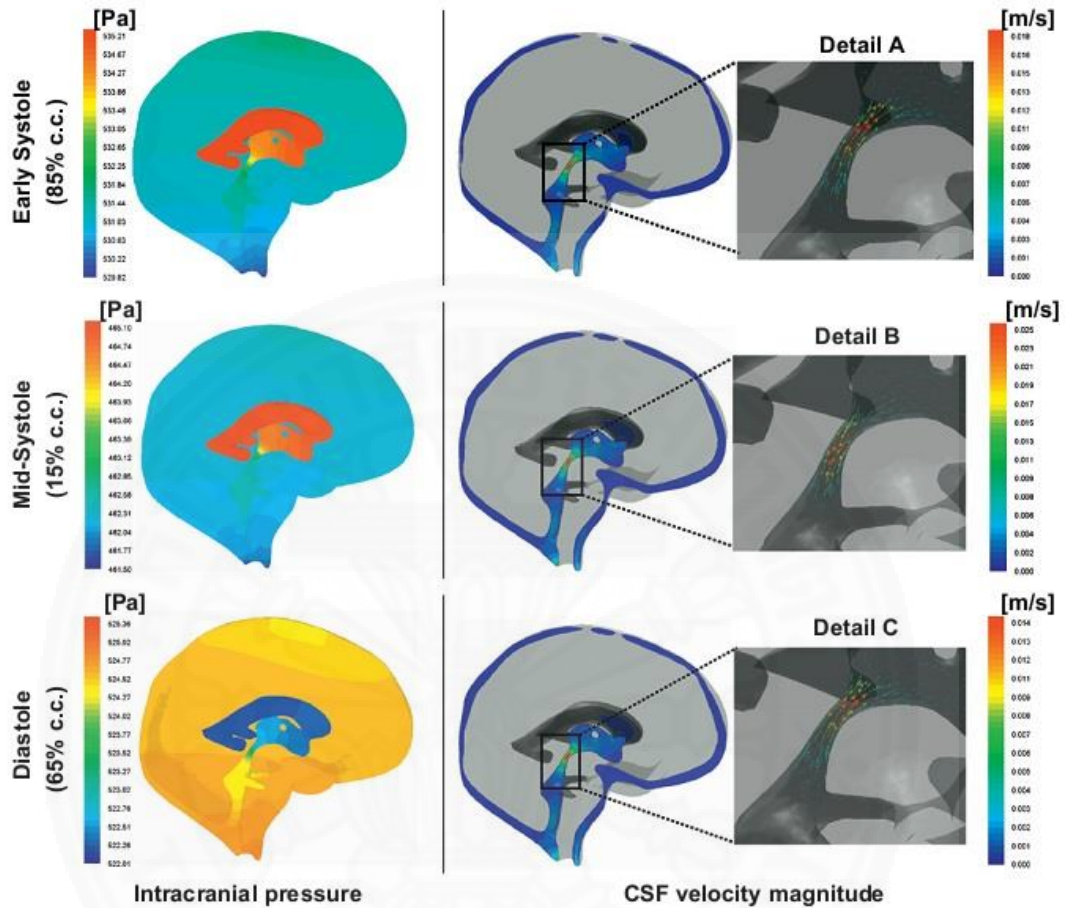
Figure 2.4. Predicted CSF Pressure and Velocity magnitude in the ventricles and subarachnoid space (Sweetman, Xenos, Zitella, & Linninger, 2011)

Figure 2.4 shows the predicted CSF pressure and velocity magnitude in the ventricles and subarachnoid spaces as the results of Brian Sweetman et al's research work. Left panel shows the pressure contour at 15%, 65% and 85% of the cardiac cycle. Pressure is highest in the ventricles at early systole with flow in the rostral direction shows in detail (A). Flow rate reaches a maximum in mid-systole with flow out of the ventricles shown in Detail (B). During the diastole, the pressure gradient reverses and bring higher in the subarachnoid space compared to the ventricles. Accordingly CSF flows back to the ventricles as shown in Detail (C).

Since brain geometry is different from patient to patient, predictions based on one solid model is not correct for everyone. To make a more accurate

14

computational modeling Andreas A. Linninger at al. (Linninger, et al., 2007) developed a 3D model based on patient's individual brain geometry as shown in Figure 2.5. They used MRI techniques to accurately measure brain geometry and the CSF flow velocities in selected regions and image reconstruction has used to obtain dimensions of the CSF pathways and the brain. It also converts the patient specific MR data into accurate two or three dimensional (3-D) surfaces and volumes. The agreement of the experimental MRI flow field with the CFD predictions demonstrates that detailed mechanistic picture of fluid flows and pressures that cause intracranial dynamics is correct.
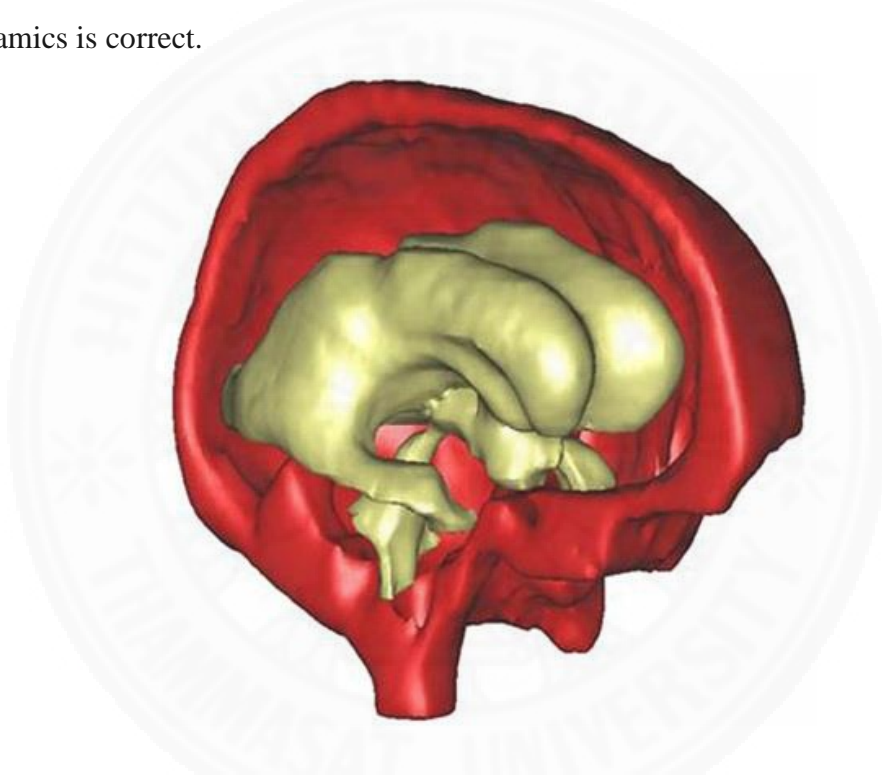
Figure 2.5. Three dimensional Reconstruction of the CSF Pathway for a Hydrocephalic patient. Ventricular system (Yellow), Cerebral SAS (Red) (Linninger, et al., 2007)

According to the Brian Sweetman et al. (Sweetman, Xenos, Zitella, & Linninger, 2011) computational results, it showed maximum CSF pressure occurred at Cerebral Aqueduct. Identification of dynamic behavior and pressure variation of CSF through the cerebral aqueduct is more important to predict the Hydrocephalus pathology.

Jeong Hyun Lee at al. (Lee, et al., 2004) contributed to quantification of CSF flow through the cerebral aqueduct in normal volunteers using phase contrast

cine MR imaging. They investigated CSF hydrodynamics of eleven healthy volunteers (mean age = 29.6 years) by 1.5T MRI system and map the velocity and Pressure variation. Results: The mean peak systolic velocities showed a tendency to increase from the superior to the inferior aqueduct, irrespective of the background baseline region, with the range being from 3.30 cms^{-1} to 4.08 cms^{-1}. However, these differences were not statistically significant. In the case of the mean flow, the highest mean value was observed at the mid-portion of the ampulla 0.03 cm3s^{-1} in conjunction with the baseline region of interest (ROI) at the anterior midbrain. However, no other differences were observed among the mean flows according to the location of the cerebral aqueduct or the baseline ROI.

As a solution of problems encountered in 3D modeling of brain J.M. Furlan et al. (Furlan, Kadambi, Loparo, Sreenath, & Manjila, 2008) used Rapid Prototyping Technique to create geometrically realistic ventricular model. In order to characterize the flow of cerebral spinal fluid (CSF) within the third ventricle and cerebral aqueduct of a healthy adult, an in-vitro steady flow loop is developed. Particle image velocimetry (PIV) is used to attain 2D velocity vector maps of the flow in the mid-sagittal plane of the model for the cranio caudal as well as caudo cranial flow directions. CSF steady flow rates used correspond to the physiological flow rate range. The PIV results demonstrated that the highest velocities occur in the mid-aqueduct region of the test section and the lowest velocities occur in a dead zone located in the antero-inferior region of the third ventricle. In the case of cranio-caudal flow, the results show a relatively small recirculation region located adjacent to a downward jet resulting from the influx of CSF from the Foramen of Monro. The results of this study have implications with respect to pathophysiology of Normal pressure hydrocephalus, mechanisms of CSF diversion in shunt surgery and Endoscopic Third ventriculostomy (ETV), targeted drug delivery via CSF, and verification of CFD models of CSF flow.

Their major objective was to measure the velocity field in a realistic geometry of the 3rd ventricle and aqueduct using PIV. This was achieved by developing and taking measurements in an anatomically accurate, 3:2 scale in vitro model of the 3rd ventricle and cerebral aqueduct regions. Velocities as low as 10

ms^{-1} - 5 ms^{-1} were mapped successfully using this technique. This study has demonstrated the crucial importance of using realistic geometry in the study of CSF flow through the ventricular system, and hence, it is highly recommended that only such anatomically accurate models be used in the characterization of ventricular flow regimes and evaluation of pathological changes in normal pressure hydrocephalus. The flow regimes investigated in this study will have implications on drug delivery, shunting practices, and ETV procedure. Specifically, conclusions of their study was:

- The flow regime measured in the cranio-caudal direction is very different from that of the caudo cranial direction. While the same antero inferior third ventricle dead zone was seen in both directions, the two recirculation regions seen in the cranio-caudal direction were not present in the caudo-cranial direction. This is due to the smooth, gradual volume increase associated with the neck of the aqueduct. Because of the diffuser-like nature of this opening, flow decelerates in a uniform manner when entering from the aqueduct into the third ventricle, hence preventing the formation of recirculation regions like the ones seen with flow in the opposite direction, where CSF enters through an abrupt opening into the 3rd ventricle.

- Recirculation regions and dead zones were identified in the third ventricle. Such regions have an impact with respect to central nervous system drug delivery, and in particular, to chemo therapeutic drugs used in the treatment of cancer. CSF administered drugs which may remain in such entrapment areas would be present for a great deal longer after intra ventricular infusion resulting in a greater degree of diffusion through the ependymal cells and into brain extra cellular space. The surfaces of ventricular walls which lie adjacent to dead zones would be expected to experience diffusion for prolonged periods of time.

- The highest velocities were measured in core region of the upper area of aqueduct of Sylvius Although study was conducted for steady flow rates only, it is believed that some of these results can extend to the dynamic flow situation (pulsatile CSF flow) that is encountered in vivo.

17

Specifically, the presence of the dead zones and recirculation regions found in this study would most likely exist in a dynamic flow regime.

As the CSF circulation process directly effect to the normal pressure hydrocephalus it is obvious, the easiest way to identify the normal pressure hydrocephalus patients is thoroughly identification of CSF circulation scenario. Cause it gives extensive explanation about the diagnosis. Intendant of this study is to develop a mathematical model to predict the dynamics behavior of CSF bulk circulation and its malfunctions across the spinal aqueduct and validate the results by computer simulation (CFD). By referring the results given by mathematical model it would be help full for doctors to predict whether patient suffering the initial stage of hydrocephalus or not. And also it will address the developing country peoples, cause its economically viable than the MRI checkup.

2.1 Review of related literature and studies

Treatment methods for hydrocephalus have not changed significantly over the past 50 years. Most patients are treated with either a third ventriculostomy or a pressure shunt; however, several shunt revisions are necessary over the course of a patient's life due to shunt malfunction or infection. This research is not about to develop or invent new treatment method thus it's an implement new normal pressure hydrocephalus disease prognosis method which based on the mathematical model, precise understandings about the parameters influence of Normal pressure hydrocephalus and comparing them with those in normal CSF circulation is necessary is and MRI, CT scanning clinical methods gives tremendous contribution for it. Some important parameters which can measure by MRI and CT scanning are shown below.

- To evaluate the changes of intracranial cerebrospinal fluid (CSF) dynamics in hydrocephalus (MR) CSF flow images in cases of acutely progressive hydrocephalus
- CSF flow patterns

MR images gives 2 dimensional cine phase sequences of CSF flow and evaluation of CSF flow can be accomplished by the use of cardiac gated echo MRI technique. The qualitative cine MR allows a rapid and dramatic evaluation of both normal and abnormal patients in a visual form. Quantitative evaluation via permits a more precise mapping of the follow patterns and is more sensitive in detecting fluid motion and allows calculation of CSF velocity.

Apart an above parameters, get understanding of,

- CSF flow pattern
- Cerebrospinal fluid pulse pressure
- Intracranial Volume
- Intracranial volume pressure relationships
- Measurement of intracranial compliance and pressure
- The Monro Kellie hypothesis

Are mandatory to develop a Mathematical model. Since CSF flow is synchronized with the cardiac pulsatile motion, it is important to prospect of Windkessel function and it's influenced to the CSF circulation.

2.2 Important Parameters has been considered

2.2.1 Windkessel Function of the Human Aorta

Windkessel effect refers to the compliance of the aorta with the arterial pressure wave, produced by the ejection volume from the left ventricle (LV). The measured systolic arterial blood pressure is largely a function of this. With atherosclerosis, the aorta stiffens and cannot absorb the pressure wave by expanding a bit. The result is that the pressure wave is less damped and carries though to the peripheral arteries where it manifests as elevated systolic blood pressure. This condition can also lead to LV enlargement and various degrees of heart failure due to increased arterial resistance. This will feed back to the RV. The most common cause of RV failure is LV failure. The failing heart will also be reflected in a rising diastolic arterial blood pressure. Large arteries like aorta and its branches have high elasticity. When blood is pumped into these vessels by heart during systole, the vessel expand to accommodate some excess blood temporarily. During diastole, when heart is not pumping, their elastic walls recoil and blood in them is propelled forward. These

19

phenomenon of Windkessel effect can be used to define the CSF pulsatile behavior at sub arachnoid spaces.

2.2.2 Cerebrospinal fluid pulse pressure and intracranial volume pressure relationship

The rapid fluctuations in the cerebrospinal fluid (CSF) pressure synchronous with the heart beat (CSF pulse) have for a long time excited the interest of numerous workers. This interest concerns the origin site of transfer, configuration, and magnitude of the pulse as well as its role in the pathogenesis and diagnosis of intracranial disease. The CSF pulse pressure is a pressure response to the transient increase in intracranial blood volume. During a cardiac cycle intracranial volume pressure (pulse pressure) increases with rising intracranial pressure (ICP).

2.2.3 Dynamic Brain Phantom for Intracranial Volume Measurements

Knowledge of intracranial ventricular volume is important for the treatment of hydrocephalus; Current monitoring options involve MRI or pressure monitors. However, there are no existing methods for continuous cerebral ventricle volume measurements. In order to test a novel impedance sensor for direct ventricular volume measurements, in order to measure the intracranial volume, 3D modeling method that developed by Sukhraaj S et al. (Sukhraaj, Harris, & Linninger, 2011) can be used to emulate the expansion of the lateral ventricles seen in hydrocephalus. Dynamic volume and pressure measurements would provide more accurate volumetric measurement of ventricular system correspond to the occasion. Figure 2.6 shows the deformation patterns of the ventricular system in hydrocephalus which has been analyzed by using 3 dimensional dynamic brain phantom.
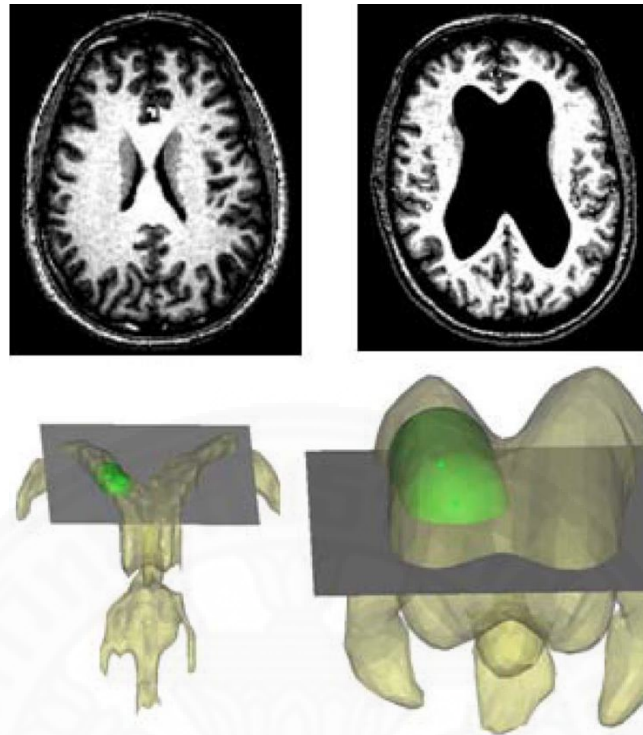
Figure 2.6. Deformation patterns of the ventricular system in Hydrocephalus. (Left) 3D reconstructions of the ventricles shown a normal subject and (Right) Patient with Hydrocephalus with the MR image s shown on the top (Sukhraaj, Harris, & Linninger, 2011)

2.2.4 Measurement of intracranial compliance and pressure by MRI

Although MRI CSF flow studies provide quantitative measures of the CSF flow dynamics, clinical utilization of these studies has been limited due to the difficulty in interpreting these measurements and due to large individual variability, even among healthy subjects. Establishing a relationship between CSF pulsation and important clinical physiological parameters such as intracranial compliance and pressure may therefore enhance the clinical role of CSF flow studies. A noninvasive method for characterization of the intracranial physiology through measurements of blood and CSF flow has been recently described. This method provides simultaneous measurements of total cerebral blood flow (TCBF), intracranial compliance, and intracranial pressure (ICP). These physiological parameters characterize the hemodynamic and hydrodynamic states of the craniospinal system.

2.2.5 The Monro-Kellie hypothesis: applications in CSF volume depletion

More than two centuries ago, Alexander Monro applied some of the principles of physics to the intracranial contents and for the first time hypothesized that the blood circulating in the cranium was of constant volume at all times (cranium was a "rigid box" filled with a "nearly incompressible brain" and that its total volume tends to remain constant). This hypothesis was supported by experiments by Kellie. In its original form, the hypothesis had shortcomings that prompted modification by others. What finally came to be known as the Monro-Kellie doctrine, or hypothesis, is that the sum of volumes of brain CSF, and intracranial blood is constant. The doctrine states that any increase in the volume of the cranial contents (e.g. brain, blood or cerebrospinal fluid), will elevate intracranial pressure. Further, if one of these three elements increase in volume, it must occur at the expense of volume of the other two elements. An increase in one should cause a decrease in one or both of the remaining two.
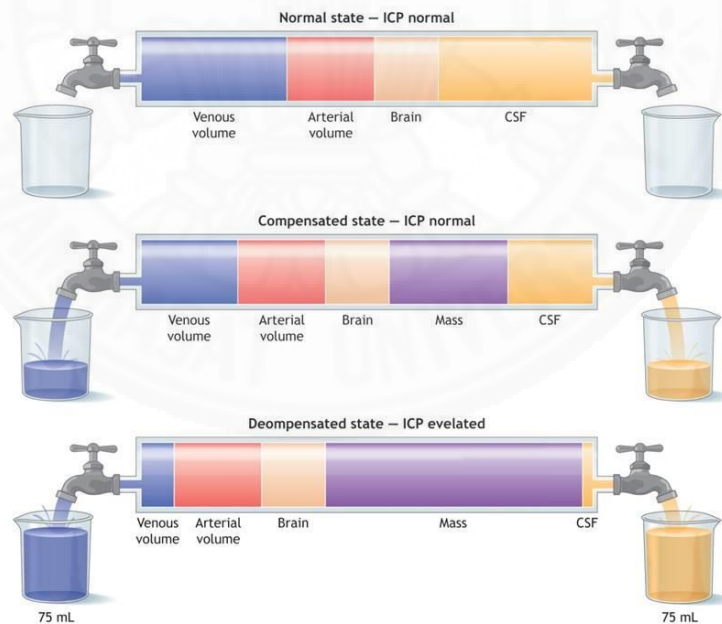
Figure 2.7. Monro-Kellie Doctoring: cranium is a rigid box filled with a nearly incompressible brain and that its total volume tends to remain constant (Monro kellie, n.d.)

Figure 2.7 describes how volume regulation of brain occurred according to the Monro-Kellie hypothesis.

This hypothesis has substantial theoretical implications in increased intracranial pressure and in decreased CSF volume. Many of the MRI abnormalities seen in intracranial hypotension or CSF volume depletion can be explained by the Monro-Kellie hypothesis.

These abnormalities include meningeal enhancement, subdural fluid collections, engorgement of cerebral venous sinuses, prominence of the spinal epidural venous plexus, and enlargement of the pituitary gland.

With the development of computational simulations and its subroutines, image processing (Reconstruction) methods has been introduced to develop 3D models based on the 2D images. MRI Imaging and Image Reconstruction and Tetrahedral mesh generation introduced into image reconstruction tools and reconstruction involves the physiologically accurate interpretation of the different substructures of the brain as well as to give meshed 3D model for the simulations.

2.3 Numerical modeling of CSF dynamic and Velocity

Under the normal physiological condition, CSF maintains a pulsatile flow of motion due to systolic expansion and constriction of the intracranial arteries causing constriction and dilation of ventricles simultaneously (Masoumi, et al., 2010). During the systole and diastole, CSF shows antagonistic pulsatile motion with respect to cardiovascular pulsation and flows in bulk with each cardiac cycle. Greitz D. (Greitz, Cerebrospinal fluid circulation and associated intracranial dynamics. A radiologic investigation using MR imaging and radionu clide cisternography, 1993) has shown, flow sensitive MRI authenticate that bulk flow of CSF excreted in cerebral aqueduct. Monro-Kellie hypothesis states that, skull is enclosed container consistence with brain (80%), intracranial blood (10%), cerebrospinal fluid (10%), and sum of the volumes of these three components are constant. Increment or decrement of volume in either one of these contents must be compensate by reducing or increasing in volume of other contents. CSF and intracranial blood can easily adapt to compensate the volume changes. If this compensatory mechanism is exhausted, further change of volume of one content can leads to rise or decrees of intracranial pressure (ICP) (Luetmer, et al., 2002), (Dunn, 2002). Overproduction or inadequate re-absorption of CSF and disorders in CSF pathway (cerebral aqueduct) will result in over

accumulation of cerebrospinal fluid in ventricles result in enlargement of brain and can be the cause of disease in ICP and hydrocephalus. Under these circumstances, better understanding of CSF dynamic, regulation of cerebral blood flow (CBF) and its waveform are helpful for the prognosis of diseases associated with cerebrospinal fluid.

In 1978, A. Marmarou et al. (Anthony, Kenneth, & Roberto, 1978) bring forwarded an important hypothesis for kinetic of the intracranial pressure. The time course was measured based on four parameters; intracranial compliance, dural sinus pressure, resistant to absorb CSF and cerebrospinal formation and role of each parameter to governing the dynamic equilibrium of ICP was measured. In his mathematical model; newly formed CSF (I_f) subdivided to two components; CSF retained within the SAS (I_s) and amount of CSF absorbs to venous blood arteries (I_a). Controversial circumstance of this model is they considered as CSF pressure are maintained at constant pressure. Since CSF has pulsatile nature of dynamic behaviour, constant pressure cannot be account.

Periodically, several researchers have been interpreted mathematical models for the CSF dynamics based on experimental and clinical pathological observations. Hakim et al. (Hakim, Venegas, & Burton, The physics of the cranial cavity, hydrocephalus and normal pressure hydrocephalus: mechanical interpretation and mathematical model, 1976) suggest some classical concepts of physics to explain about the rational mechanics of the cranial content and shown that, how the intraventricular pressure gradient creates stress on brain parenchyma and its variation throughout the CSF production.

Mauro Ursino (Mauro, A mathematical study of human intracranial hydrodynamics part 1—The cerebrospinal fluid pulse pressure, 1988), (Mauro, A mathematical study of human intracranial hydrodynamics part 2—Simulation of clinical tests, 1988) has proceeded an A mathematical study of human intracranial hydrodynamics based on the cerebrospinal fluid pulse pressure and auto regulation. But his studied despite to consider the influence of cardiac cycle in term of the pulsatile motion of cerebrospinal fluid.

However, recently Simone Bottan et al. (Simone, Dimos, & Vartan, 2012) formed a 3D Phantom model of cranial system and analysed the physiologic

cerebrospinal fluid dynamics by considering bulk and pulsatile physiologic CSF flow. Similarly, Ambarki et al. (Ambarki, et al., 2007) developed an A new lumped parameter model of CSF hydrodynamics throughout the cardiac cycle in healthy volunteers and was able to analyse the time domain characteristics including time shift of arterial and CSF flow.

In the contest of CSF pulsatile motion analysis, the hypothesis of Linninger et al. (Linninger, et al., 2005) plays a vital role. Their model of fluid structure interactions was able to predict the flows and pressures patterns throughout the brain's ventricular pathways and quantifies the pulsatile CSF motion including flow reversal in the cerebral aqueduct.

In this context, we developed a mathematical model to imply the pulsatile motion of CSF through the cranial space based on the analogy of arterial dilation and contraction. Main advantage of this method is been a non-invasive method. Monitoring and cognizance of parameters of CSF like, flow pattern, periodicity and flow rate helps physicians to systematically analyse and diagnosed the disorders associated with intracranial hydrodynamic of any patient by comparing with normal physiological condition.

In this comprehensive study, we paid our attention for deeper insight of dilation and contraction of blood vessels, mechanical forces exerted on the blood vessel inner wall while using basic principles of fluid mechanics and theory of spring damper analysis. Conclusively emphasis, CSF pulsatile motion is dominantly driven by dilation and contraction of arteries due to its pulsatile motion of blood. The source of our study was the former retrospective study of "Pulsatile Cerebrospinal Fluid Dynamics in the Human Brain" by Andreas A. Linninger et al. (Linninger, et al., 2007), (Linninger, et al., 2005). Their model was adequate to quantify the pulsatile volumetric flow motion of CSF through the cerebral aqueduct.

Flow sensitive MRI investigations has shown, CSF flows as bulk in each cardiac cycle and most prompt CSF bulk flow occurred in our ROI (Egnor, Zheng, Rosiello, Gutman, & Davis, 2002), (Greitz, Cerebrospinal fluid circulation and associated intracranial dynamics. A radiologic investigation using MR imaging and radionu clide cisternography, 1993). The bulk flow velocity of CSF deduct to the ratio of 3:1 by aqueduct in order to maintain continuous flow to the site of cranium space

(Naidich, Altman, & Gonzalez-Arias, 1993). These results was increased our curiosity to make a math model for understand the physiological phenomenon of cerebral aqueduct by selecting as region of interest. Clear understanding on phenomena of CSF driving force and its flow pattern helps physicians to discriminate abnormalities with the normal physiological conditions.

2.3.1 Arterial compliance

Active transportation of blood in human beings is primarily governed by the cardiac cycle. The blood circulatory system is a closed organon and transport blood from the heart to capillaries and capillaries to heart in unidirectional way. Arterial vessels are not totally rigid and its elastic nature conduced forth and continuous motion of blood by disrupting the reverse motion. Oscillatory movements of blood flow enlarge the elastic artery resultant of systolic flow induced pressure and facilitate an accommodation for additional blood volume. Diastolic recoil of arterial wall thrust the additional blood volume and maintains continuous blood flow to the forth during systole and diastole. The mechanism is also known as the Windkessel effect which has introduced by Otto Frank (Otto, 1899). Relationship between volumetric changes of arterial blood (ΔV) due to the particular arterial blood pressure change (ΔP) can be quantified as compliance (C) (Spencer & Dennison, 1963).

$$C = \Delta V / \Delta P \qquad (2.1)$$

For assessments, cross-sectional compliance (CC) is considered due to the inappreciable amount of strain along the longitudinal direction of blood vessel and volumetric change is evaluated in radial direction. Cross-sectional compliance interprets as the ratio of arterial cross-sectional area (ΔA) to pressure difference (ΔP) (Reneman, Merode, Hick, Muytjens, & Hoeks, 1986).

$$CC = \Delta A / \Delta P \qquad (2.2)$$

Arterioles are form with endothelium and vascular smooth muscles. These two layers exhibit stiff and springy properties by elastin vessel to sustain in higher

26

pressure. Vascular smooth muscles respond even for a small pressure drop by stretching the diameter and, change of diameter can dramatically influenced to the adjustment of arterial blood flow resistant. By assuming that blood flow is steady and vessel is rigid and uniform, resistant of blood flow can be computed using Hagen Poiseuille's rational.

$$R_{Arterial} = 8\eta L / \pi r^4$$
(2.3)

{Where; η is blood viscosity, L-length of blood vessel and r is radius}

Arterial compliance balance the pressure gradient corresponds to the variation of $R_{Arterioles}$. Under the normal physiological condition of young healthy person, pulsatile blood pressure fluctuates between 80 mmHg diastolic and 120 mmHg of systolic pressure. To the mathematical applications, mean arterial pressure (MAP) is considered as the average driving pressure and can be calculated as,

$$MAP = P_{Diastolic} + (1/3)(P_{Systolic} - P_{Diastolic})$$
(2.4)

2.3.2 Former model by Linninger et.al

The model proposed by Linninger et.al. (Linninger, et al., 2005) followed the first principles of fluid dynamics in order to calculate CSF pressure and velocity variation over the brain. They treated as; kinetic energy of arterial compression on the choroid plexus is basically affected to the pulsatile motion of CSF dynamic and brain parenchyma gives a feedback to its auto-regulation. To simplify the complexity of mathematical application, one dimensional framework has used. Navier-Stocks and momentum equation were used to acquire the fluid dynamics results and some of elastostatic laws were used to compute stresses and strains on brain parenchyma. Fig. 2.8 shows the model which is illustrating of ventricles and its displacement due to the forces act on elastic brain tissues.
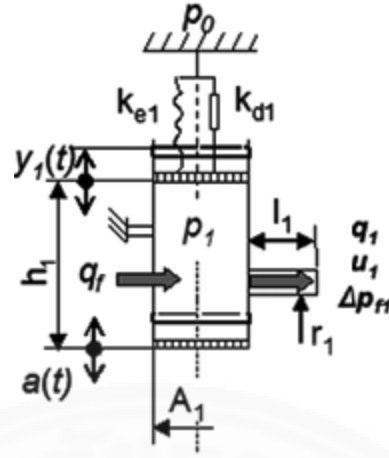
Figure 2.8. Forces imparted on ventricles and its displacement (Linninger, et al., 2005)-edited. Linear elastic springs represent the periventricular tissues

To quantify the parenchymal tissue deformation, the standard thin elastic membrane model of Brooks et.al. (Brook, Falle, & Pedley, 1999) were only considering epithelial layer in the peri-ventricular area. The pressure difference between CSF pressure in ventricles (p_i) and pressure of brain parenchyma (p_o) caused to the expansion of ventricular wall. The acceleration of membrane element showing in Fig. 2.8 employed by three forces; pressure difference of CSF and brain tissues (p_i-p_o), epithelial tissue elasticity ($k_e.y_i$) and dissipative force ($k_d.\dot{y}_i$). Inside of ventricles are filled with cerebrospinal fluid and compressed the walls due to the inbuilt pressure. Oscillatory motion of choroid expansion and contraction synchronized with the cardiac cycle and presented as the force function;

$$a(t) = \alpha \left(1.3 + \sin\left(\omega t - (\pi/2) - 0.5\cos\left(2\omega t - (\pi/2)\right)\right)\right) \qquad (2.5)$$

Important fact is, foramen of monro was considered as an elastic tube. Moreover, average axial velocity (v_i) has counted for the moment balance and radial moment balance were neglected. The rate of change in tissue deformation ($\dot{y}_i$) is equate to the radial velocity and volumetric change has quantified by $A.\dot{y}_i(t)$. According to the basic principles of the hydrodynamics, fluid flows from region of high pressure to region of low pressure. In fact, CSF flows from ventricles to veins

where it is absorbed. Kinetic of CSF is betiding as a result of pressure drop among the SAS and arachnoid villi.

By applying newton's second law of motion for the equilibrium condition of motion under the three forces; force exerted on the ventricular wall due to the pressure difference (P_i-P_o), elastic tissue compliance ($k_e.y_i(t)$) and dissipation by first order damping force ($k_d.\dot{y}_i(t)$). Acceleration of brain parenchymal tissues was derived as in 2.6.

$$(\rho_\omega A_i \delta)\ddot{y}_i(t) + k_d \dot{y}_i(t) + k_e y_i(t) - A_i[p_i(t) - p_o(t)] = 0 \qquad (2.6)$$

$$i \in \{LV_1 - LV_4, SAS\}$$

Continuity of cerebrospinal fluid throughout the ventricles was derived as;

$$\partial\{A_i[h_i + a(t) + \dot{y}_i(t)]\}/\partial t = q_{f,i} - q_i \qquad (2.7)$$

$$i \in \{LV_1 - LV_4\}$$

Axial moment upon the foramen of monro,

$$\rho[(\partial v_i/\partial t) + v_i(\partial v_i/\partial z)] + \partial p_i(t)/\partial z = -F_i \qquad (2.8)$$

$$i \in \{FM, AS, FL\}$$

Where, $F_i = (8\mu/r_i^2)v_i$

All the equations were solved in Laplace domain by the Simulink MATLAB platform and characteristic mechanical properties of CSF and tissues used to compute the equations are tabulated in Table 2.1.

After computing the math model, they have seen maximum velocity occurred through the aqueduct of Sylvia as +25.8 mm/s and -21.7 mm/s. Nevertheless, literature values of CSF velocity via the aqueduct of Sylvia based on the clinical observations shows a deviation from this value (Naidich, Altman, & Gonzalez-Arias, 1993), (Enzmann & Pelc, 1993), (Marco, et al., 2004), (Haughton, Korosec, Medow, Dolar, & Iskandar, 2003).

Despite the fact that many hypothesis have exhibited, non-of explain how mechanical energy of blood pulsatile motion transmit to the CSF motion. Since, blood circulatory system is fully enclosed circuit, there might not be any fluid interaction between cerebral blood and CSF accept in the venous blood at arachnoid villi.

Table 2.1: characteristic mechanical properties of CSF and tissues

Property	Value
Young Modulus for ventricles	2,100 N/m^2
Young Modulus for SAS	3,500 N/m^2
CSF density, ρ_f	1,004-1,007 kg/m^3
Density of blood , ρ_B	1025 kg/m^3
CSF Viscosity, μ_{CSF}	10^{-3} Pas
Ventricular tissue Spring elasticity, k_e	8 N/m (Normal)
Brain tissue Dampening , k_d	0.35×10^{-3} (Ns)/m
Spring elasticity of Arterioles , k_B	10 N/m (Assume)
Ependyma density , ρ_ω	1,000 kg/m^3
Reabsorption constant, k	1.067×10^{-11} m^3/(Pas)

Chapter 3
Methodology

3.1 Numerical analysis- Transmit of mechanical energy from arteries to CSF

In this hypothesis, we bring forward that CSF pulsation dominantly occurs due to the pulsatile movement of blood. Mechanical energy dissipates during the dilation and contraction of blood vessel transmits to ventricular system in order to generate oscillatory motion of CSF. Arteriole wall and ventricular tissues were substitute in to two elastic springs and connected each in series. Few assumptions have made as; springs are frictionless, massless, springs are obeying with Hooke's law and consider only in linear elastic range. Figure. 3.1 shows the model of arteriole and ventricular springs, forces exerted on arteriole inner wall and its dilation.
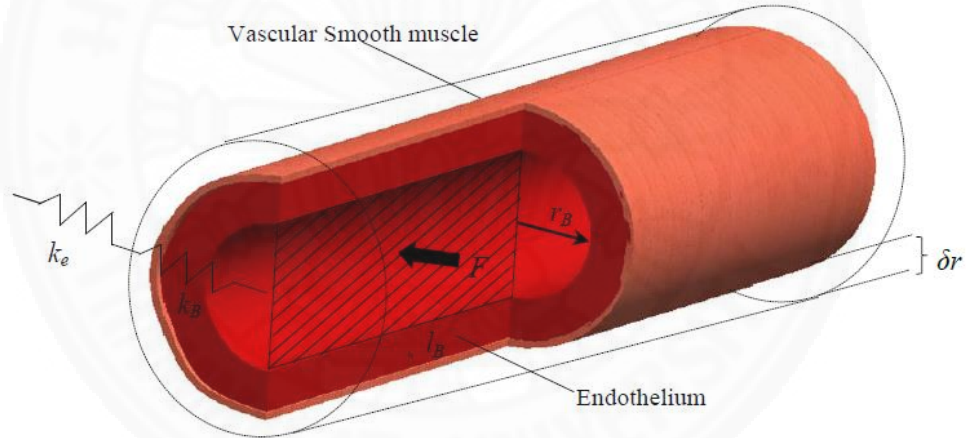
Figure 3.1. Model of Arteriole and ventricular springs

$$Q_{in} = Q_{Stored} + Q_{Out} \tag{3.1}$$

Force applies on arteriole inner wall (FB) is equal to MAP time projected area of inner wall.

$$F_B = MAP \times A_B \tag{3.2}$$

$$F_B = \left\{ P_{Diastolic} + (1/3)\left(P_{Systolic} - P_{Diastolic} \right) \right\} \times r_B \times l_B \tag{3.3}$$

For an equilibrium condition of spring system can be mathematically model as;

$$m_B \delta \ddot{r} = F_B(t) + k_B \left(y_i(t) - \delta r \right)$$ (3.4)

Newton's second law of motion has been applied to the blood element and m_B is the mass of blood element. Under the equilibrium state, m_B time acceleration of radial displacement equals to the sum of force applies on the arteriole inner wall and resultant spring force of arteriole with respect to relative displacement of arteriole and ventricular tissues.

$$m_{CSF} \ddot{y}_i(t) = -k_B \left(y_i(t) - \delta r \right) - k_e y_i(t)$$ (3.5)

By applying Newton's second law for the ventricular tissue spring, equilibrium can be stated as in equation 3.5. For system balance, two equations can be written in matrix form,

$$\begin{pmatrix} m_B & 0 \\ 0 & m_{CSF} \end{pmatrix} \begin{pmatrix} \delta \ddot{r} \\ \ddot{y}_i \end{pmatrix} + \begin{pmatrix} k_B & -k_B \\ -k_B & (k_B + k_e) \end{pmatrix} \begin{pmatrix} \delta r \\ y_i \end{pmatrix} = \begin{pmatrix} F_B(t) \\ 0 \end{pmatrix}$$ (3.6)

MATLAB Simulink has been used as mathematical platform to plot the displacement of ventricular tissues with respect to the displacement of arteriole wall. Unit impulse input was applied. Quantitative values for each parameter are showing in Table 3.1 and elastic constant for an arteriole has assumed as 10 N/m.

Moreover, to confirm the relevance of ventricular tissue displacement and CSF velocity through the aqueduct, we defined a simple model for the CSF trapped in ventricular cavity as Figure 3.2. For a normal healthy person, ventricular cavity accommodates 25-30 ml of CSF in one time. In this approach we liken ventricular cavity as a sphere with one degree of freedom to deform and considered the volume of CSF in ventricle at one time as 27.5 ml. Radius of model sphere (r_{Sphere}) for 27.5 ml volume is 18.72 mm. Since ventricular cavity is enclosed volume, same amount of

CSF with respect to the volumetric displacement due to the y_i should leave from the site. Aqueduct of Sylvia acts as the passage way to escape the displaced volume of CSF. According to the cine phase MRI studies of Hueng et.al (Hueng, et al., 2011), cross sectional area of aqueduct ($A_{aqueduct}$) has given as 3cm². By examine relevant parameters, velocity of CSF through the aqueduct ($V_{CSF\,aqueduct}$) for a normal subject can be mathematically modelled as;

$$A_{aqueduct} \times V_{CSF\,aqueduct} = (4\pi/3)\left\{r_{Sphere}^{3} - \left(r_{Sphere} - y_i\right)^{3}\right\} \tag{3.7}$$
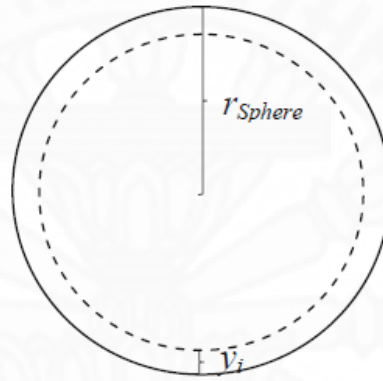
Figure 3.2. Ventricular cavity assigned as sphere

3.2 Computational Fluid Dynamic Analysis

Very less number of researches has been done analogous to the CFD analysis of ventricles. But, attributed aspects by Brian J. Sweetman (Sweetman B. J., 2011) is salient. A Two-dimensional simulation of the CSF flow field at mid systole in a sagittal brain section of normal and hydrocephalic subjects has been done. Computational fluid dynamics simulations and clinical MRI measurements, based on six normal and five communicating hydrocephalic subjects (Linninger, et al., 2005), (Linninger, et al., 2007). Compared in detail are the CSF flows in two regions of interest - in the aqueduct of Sylvius and in the pre-pontine area. In normal subjects, the flow velocity amplitude is much higher in the pre-pontine area than in the aqueduct. In hydrocephalus, the aqueduct flow is increased, while the velocity in the pre-pontine area is reduced. The ratio of the aqueduct to the pre-pontine velocity

amplitude is about seven times larger in hydrocephalic cases than in normals. This change suggests that the ratio of the pre-pontine to the aqueduct flow amplitude could be an indicator for the status of communicating hydrocephalus. While this ratio has not been used for diagnosis yet, its significance might be confirmed in future research. Figure 3.3 shows snapshots of simulated velocity fields at the peak of the systole using patient-specific lateral brain sections of a normal and a hydrocephalic subject, where a two dimensional simulation of the flow field is created as previously published. The discussion will present a mechanistic explanation for these changes in the flow patterns occurring in hydrocephalus.
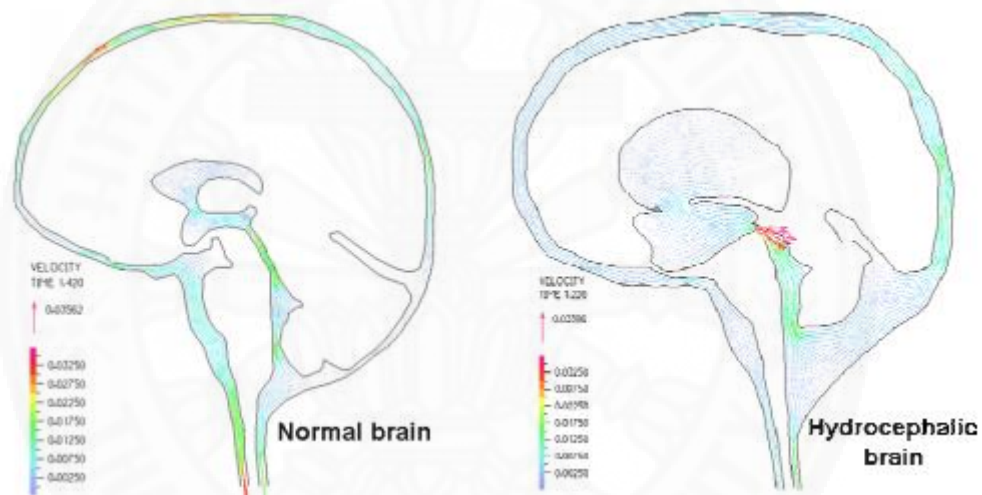
Figure 3.3. Two-dimensional simulation of the CSF flow field at mid systole in a sagittal brain section of normal (left) and hydrocephalic subjects (right) (Sweetman B. J., 2011)

As their recommendation for the future research, this CFD analysis was highly focused on CFD analysis of CSF attributed with buffering effect of ventricular system and exact morphometric shapes of aqueduct of Sylvia. Computational fluid dynamics analysis has done to identify the dynamic behavior of CSF through the aqueduct for a normal patient and Normal pressure hydrocephalus case. Geometric information of aqueduct was taken from the three controlled subjects which admitted to Thammasat Hospital. Patients were 29 to 52 years of age (35%male and 65% Female). Retrospective results of numerical modeling has been used as initial data for ANSYS CFX analysis. The aim of this comprehensive study is to quantify the

velocity variation of cerebrospinal fluid (CSF) for narrowest point in aqueduct of Sylvia (AqSylv) of normal patients and normal pressure hydrocephalus (NPH) patient by corresponds to its concave shapes of anteriorly and inferiorly. T2-weighted 3-T magnetic resonance images (MRI) of head in DICOM (Digital Imaging and Communications in Medicine) format were taken from three controlled patients whose were admitted to Thammasat Hospital, Thailand. Patients were 29 to 52 years of age with two normal patients and one (NPH) patient. DICOM files were three dimensionally re-constructed by using 3D slicer software, and geometric information of aqueduct for all three cases has been noted. Solid models of aqueduct for both normal patient and NPH condition were developed by based on the geometric information. Computational fluid dynamics (CFD) analysis has been done to quantify the CSF velocity variation throughout the narrowest point of aqueduct for both cases of normal and NPH condition. Retrospective results of "Mathematical model for dynamics of CSF through the aqueduct of Sylvia based on an analogy of arterial dilation and contraction" has been used as initial data for ANSYS CFX analysis. Results showed that CSF moves through the aqueduct in sinusoidal pattern in both cases. At the narrowest point of aqueduct, amplitude of peak CSF velocity for NPH patients is significantly higher than the amplitude of peak CSF velocity for normal patient. CSF velocity variation throughout the aqueduct co-relates with the pressure gradient inside the aqueduct and increases in the third ventricle direction.

The aqueduct of Sylvia (AqSylv) is a tube which connects third and fourth ventricles. Investigations of Lindgren and DI Chiro (Lindgren & Di Chiro, 1953) has shown that diameter of the aqueduct is varying throughout its length and shows a shape of swan neck. Characteristics and parameters of AqSylv is more important since it acts as a passage to flow CSF from third to fourth ventricles. Any abnormalities in dimensions of aqueduct could leads to the malfunctioning in motion of CSF. Cerebral spinal fluid secretes from choroid plexus in lateral, third and fourth ventricles and enters to the subarachnoid spaces (SAS). Fig. 2.1 shows the ventricle system and CSF pathway of human brain. Since cranial volume is constant, CSF absorption by arachnoid granulations into venous circulation is inevitable circumstance and absorption rate is linearly related to the intracranial pressure (ICP) (Anthony M & Benjamin S, 2009). Monro-Kellie's doctrine represents the

compensation and auto-regulation process of cerebral blood and CSF volumes in cranial space. CSF is a colorless liquid (Masoumi, et al., 2010) and permeates from the choroid plexus at a rate of 0.2 - 0.7 ml/minute. Ventricular system accommodates 20% of CSF volume out of its total volume of 125-150 ml at a time. Dominant percentage of CSF manufactures in lateral, third ventricles and moves as a bulk flow through the AqSylv to fourth ventricle (Greitz, Cerebrospinal fluid circulation and associated intracranial dynamics. A radiologic investigation using MR imaging and radionu clide cisternography, 1993). Any obstruction in AqSylv will result in blockage of CSF continuum flow and can lead to enlargement of ventricles due to the CSF trapping inside the lateral and third ventricles, which is a symptom of congenital or obstructive hydrocephalus (Neurosurgery, n.d.), (Nervous System, n.d.).

Aqueductal stenosis narrow the cross sectional area of AqSylv and make resistance to the CSF flow. Malfunctioning in CSF motion is increased the volume of ventricles by resulting the higher inbuilt pressure inside the ventricle system and enlarge towards the skull (Spennato, Tazi, Bekaert, Cinalli, & Decq, 2013). Scientist considered that aqueductal stenosis is a root cause of non-communicating hydrocephalus, as the obstruction in aqueduct would result the accumulation of CSF in ventricles. In the communicating hydrocephalus, the lateral ventricles and medial parts of the temporal lobes expand due to accumulated CSF inside and compress the aqueduct as a consequence of volume compensation in skull. Subsequently, the pressure inside the fourth ventricle declines and cause the aqueduct to close more tightly. These phenomena is also illustrates as aqueductal stenosis, a root cause of hydrocephalus (McMillan & Williams, 1977).

CFD analysis has done to quantify the velocity variation of CSF through the AqSylv. MRI DICOM of aqueduct was taken for particular two normal patients and one NPH patient. DICOM files were exported to the 3D Slicer software and 3D models were generated. Geometric information of aqueduct which corresponds to the normal and NPH patients were noted. Measured mean morphometric of the ventricular system were, width of lateral ventricles 30 mm; length of aqueduct 14.1 mm; diameter of narrowest point of aqueduct for normal patient 0.9 mm; inclination

of aqueduct relate to the third and fourth ventricles are 26º and 18º respectively (Matys, Horsburgh, Kirollos, & Massoud, 2013), diameter of narrowest point of aqueduct for hydrocephalus patient were reported as 0.5 mm and we assumed it as 0.6mm for NPH patient. Solid models of aqueduct were built for both cases by considering the anatomical shape of concave anteriorly and inferiorly.

Computed solid models by using Solidworks© were exported to the ANSYS CFX to generate mesh, and to set up the boundary conditions. In addition to the retrospective computational fluid analysis has been done by other researchers based on the rigid wall domain for aqueduct, we considered aqueduct wall as a deformable membrane. Properties that we used are showing in Table 3.1. Navier-Stokes equations applied as the continuity of CSF though out the aqueduct. Several assumptions were made such as CSF is incompressible, viscous, homogenous and Newtonian fluid. Considering aqueduct wall as deformable membrane was more important, whereas it influenced to the pressure variation by acting as elastic buffering chamber due to its elastic properties (Giesel, et al., 3D Reconstructions of the Cerebral Ventricles and Volume Quantification in Children with Brain Malformations, 2009), (Greitz, Nordell, Ericsson, Sthlberg, & Thomsen).

Table 3.1. Characteristic properties of CSF and brain tissues

Property	Value
Young Modulus of Ventricles	$2,100$ N/m^2
Young Modulus of SAS	$3,500$ N/m^2
Density of CSF, ρ_f	$1,004\text{-}1,007$ kg/m^3
Viscosity of CSF, μ_{CSF}	10^{-3} Pas
Ventricular Tissue Spring Elasticity, k_e	8 N/m (Normal)
Brain Tissue Dampening, k_d	0.35×10^{-3} (Ns)/m
Specific Gravity of CSF	1.007

Former study results of "Mathematical model for dynamics of CSF through the AqSylv based on an analogy of arterial dilation and contraction" (Thalakotunage & Thunyaseth, 2015) used as the initiation condition of CFX analysis, and its resulted velocity profile of CSF through the aqueduct used to CFX as an expression to initial conditions.

Chapter 4

Results and Discussion

4.1 Results

According to the Simulink simulation results of equation 3.6, displacement of artery wall and ventricular tissues shows a pulsatile variation as in Figure. 4.1. $\delta r(t)$ and $y_i(t)$ represent the blood wall displacement and ventricular tissue displacement correspondingly. To simulate the model in realistic manner, impulse signal has been given to the springs as input since cardiac pulse almost similar to impulse signal.
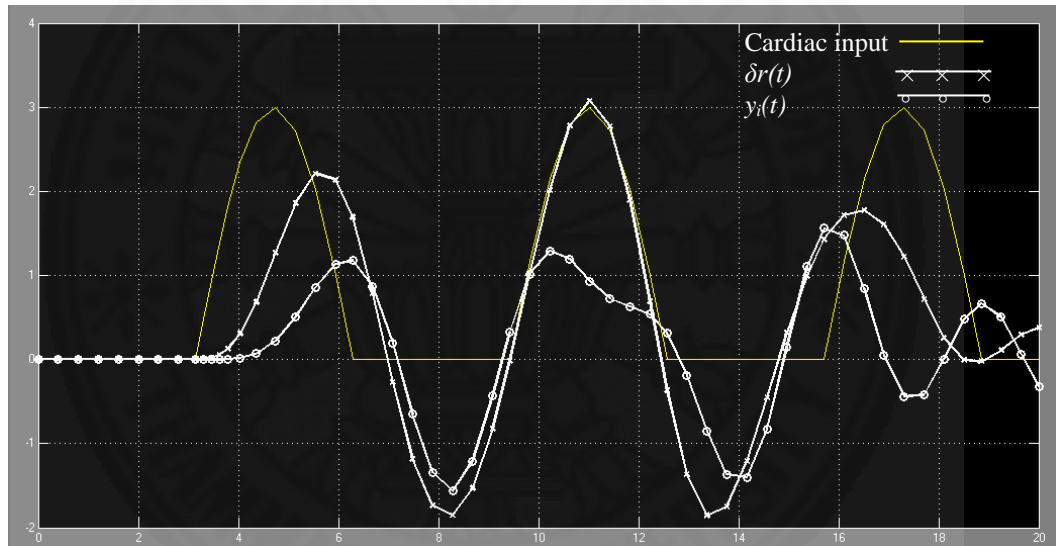
Figure 4.1. Displacement of artery wall and ventricular tissues under the pulsatile input. Vertical axis denotes the millimetre and horizontal axis denotes R-R cardiac intervals

Isomorphism of cardiac pulse wave and ventricular tissue displacement during the one single cardiac cycle benefits to validate our model, which demonstrates the correlation of blood vessel dilation and ventricular displacement in the aspect of two springs which connected in series. In addition, similarity of aqueductal CSF flow corroborates the correlation between ventricular tissue displacement and cardiac pulsatile motion.

Based on the reciprocate movement of y_i and clinical measurements of CSF velocity variation pattern; we stated that, variation of ventricular volume change

38

is proportional to the y_i. Acquired volume of ventricles due to the displacement of tissues, increase the pressure inside ventricles. To compensate the volume change, CSF in the ventricles has to be removed from ventricular space. By applying maximum ventricular tissue displacement (y_i) in to the equation 2.14, maximum velocity of CSF through the aqueduct can be calculated as 2.275 cm/sec for 1.7mm of y_i and $A_{Aqueduct} = 3cm^2$. To validate the results of math model and its correlation with Simulink results, we used real CSF velocity data's of ten healthy subjects which measured by Haughton VM et al. (Haughton, Korosec, Medow, Dolar, & Iskandar, 2003). Their results shown in Table II, the average peak systolic velocity is 2.36 cm/s. With that validation, peak systolic CSF velocity can be written as 2.2±0.2 cm/s.

Table 4.1. CSF velocity values for ten healthy subjects (Haughton, Korosec, Medow, Dolar, & Iskandar, 2003)

Volunteer No:	Age (years)	Peak Systolic velocity (cm/s)	Peak Diastolic velocity (cm/s)
1	61	2.1	2.4
2	36	1.7	2.1
3	28	2.0	1.6
4	21	2.7	4.2
5	33	2.9	1.9
6	48	1.2	2.1
7	41	2.2	4.5
8	47	2.4	2.5
9	46	3.3	3.5
10	30	3.1	2.9
Average	39.1	2.36	2.77

According to the simulation results of our model; CSF velocity pattern through the aqueduct and its correlation with ventricular tissue displacement are shown in figure. 4.2. Results shows, CSF flow velocity proportional to the ventricular displacement and CSF flow is synchronized with cardiac pulsation with making a small phase shift.
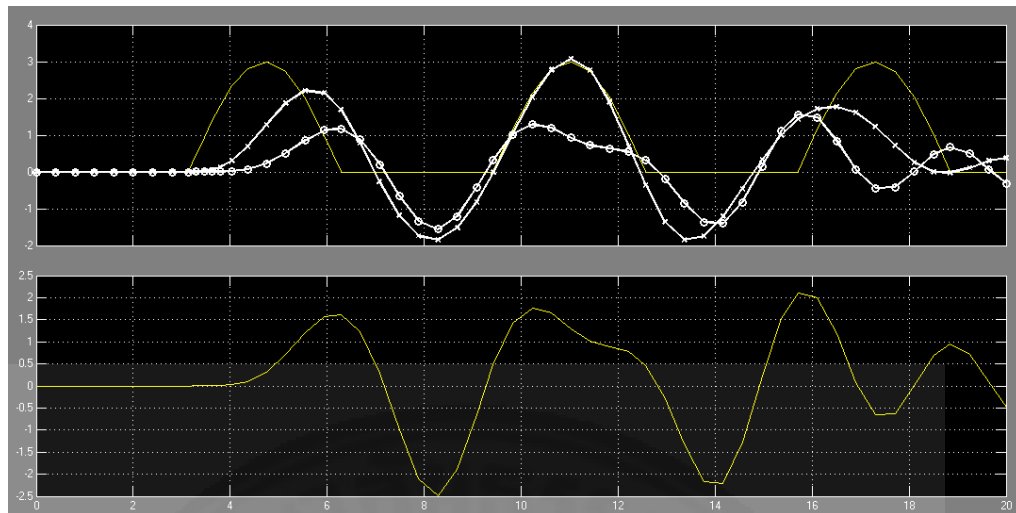
Figure 4.2. CSF velocity profile through the aqueduct with respect to ventricular tissue displacement. CSF velocity in terms of "cm/sec" in term of cardiac R-R intervals

Further, Giovanni de Marco et al. (Marco, et al., 2004) have measured net aqueductal CSF flow velocities of normal subject in three times over ten month period by using phase-contrast cine MR imaging. Aqueductal CSF velocities profiles of their clinical observation are showing in Figure 4.3, and velocity variation is similar with our simulation results during one cardiac cycle.
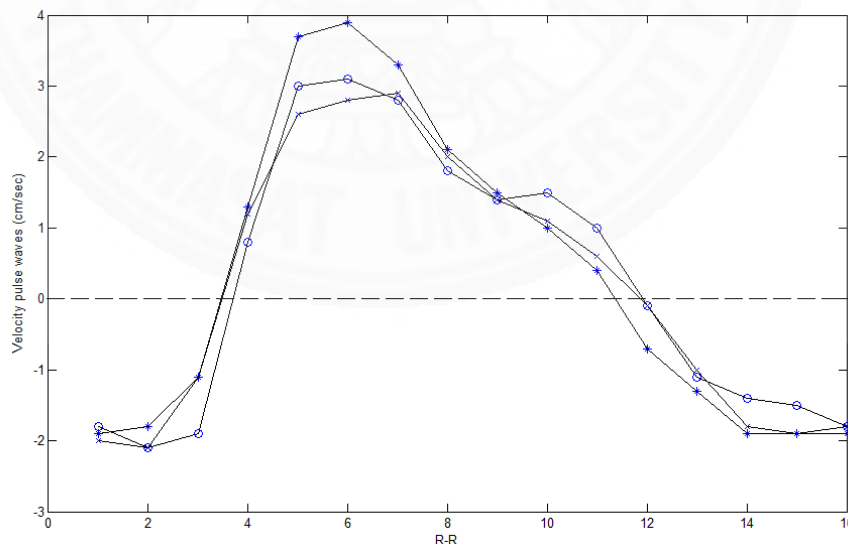
Figure 4.3. Aqueductal CSF flow velocities of normal subject in three times over ten month period (Marco, et al., 2004)-Edited.

R-R interval denotes the time interval between two corresponding ventricular depolarization. Velocities above the horizontal axis represent the CSF

flow in the craniocaudal direction and below the horizontal line represent caudocranial direction of flow (Hueng, et al., 2011).

Besides the clinical measurements, Brian J. Sweetman (Sweetman B. J., 2011) has done a simulation analyze the CSF velocity profile as shows in Figure 4.4 and his results shows similar pattern with our results.
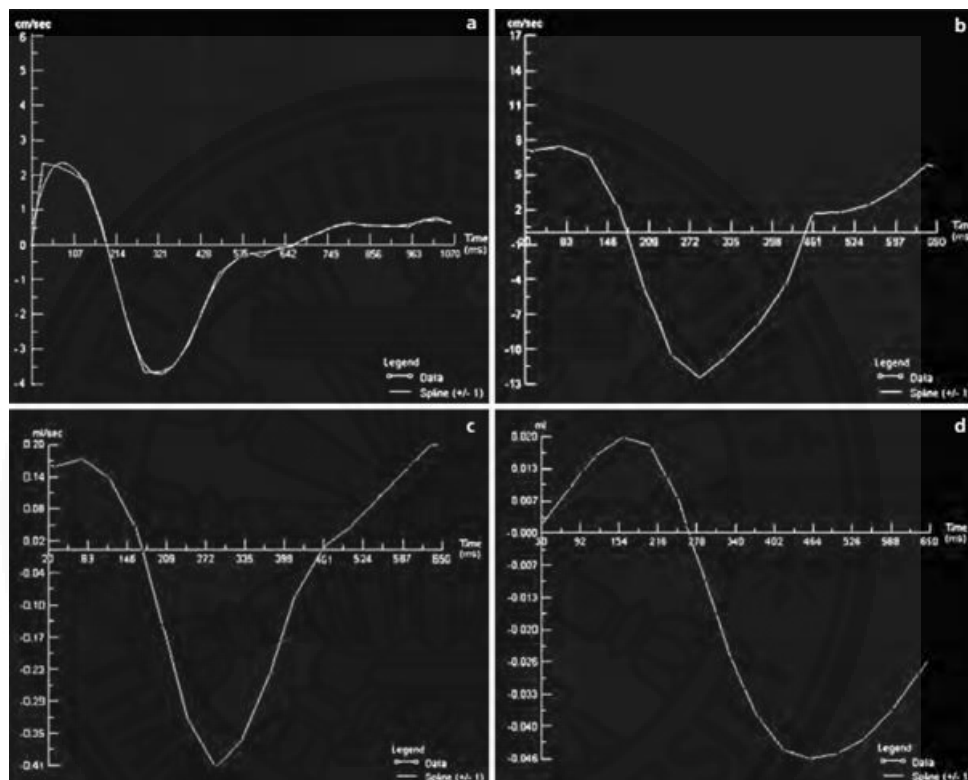
Figure 4.4. a–d. (a) Graphic showing aqueductal CSF velocity change with time in a single cardiac cycle. The area above tha baseline represents cranial velocity, while the area below the baseline represents caudal velocity. (b) Graphic showing aqueductal CSF peak velocity with time in a single cardiac cycle. (c) Graphic showing aqueductal CSF flow change with time in a single cardiac cycle. The area above the baseline represents cranial flow, while the area below the baseline represents caudal flow. (d) Graphic showing net aqueductal CSF flow in a single cardiac cycle. The curve in this graphic is different from the rest of the graphic curves; the end point of the curve gives the net flow value (Sweetman B. J., 2011)

By comparing actual clinical data of peak systolic and peak diastolic velocity of CSF and simulation results, we can conclude that governing force of CSF motion is dominantly governed by arterial wall expansion and contraction in radial direction. CSF motion is synchronized with cardiac pulsation and shows reciprocate

motion. An extensive studies of CSF dynamic behaviours helps to diagnose many diseases like Hydrocephalus, Cerebral edema, malignant infarction and subarachnoid haemorrhage etc. This math model can be used to model the CSF dynamic motion based on cardiac pulsation and further studies will leads to find diagnosis methods for particular diseases.

4.1.1 3D reconstruction of ventricle system

T2-weighted axial MRI data (in DICOM format) of 3 controlled subjects has used to develop 3D models of cerebral aqueduct for normal patients and Normal Pressure Hydrocephalus patient. 3D slicer open form software used to 3 dimensionally reconstruct the ventricular system and dimensions were taken from the reconstructed 3D models. DICOM files were imported to 3D slicer software to do the volume rendering of ventricle system, and preset as CT-coronary Artery view to investigate the dimensions and geometries of ventricle system. Figure 4.5 shows three dimensionally reconstructed model of NPH patients' ventricle system.

(a)   (b)
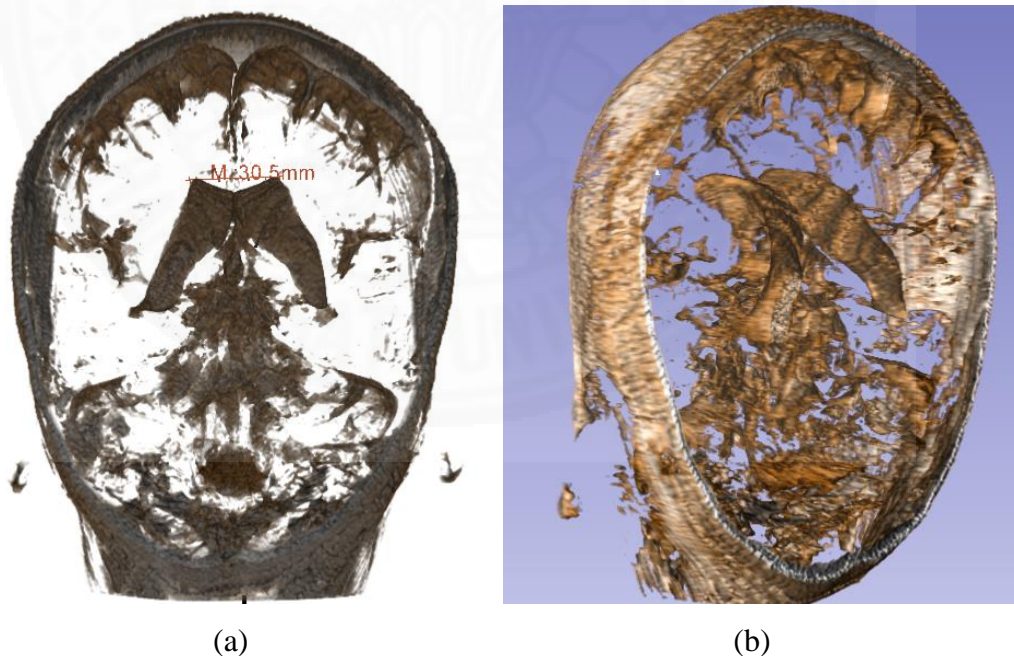
Figure 4.5. (a) and (b) shows 3D models of ventricular system for two female patients
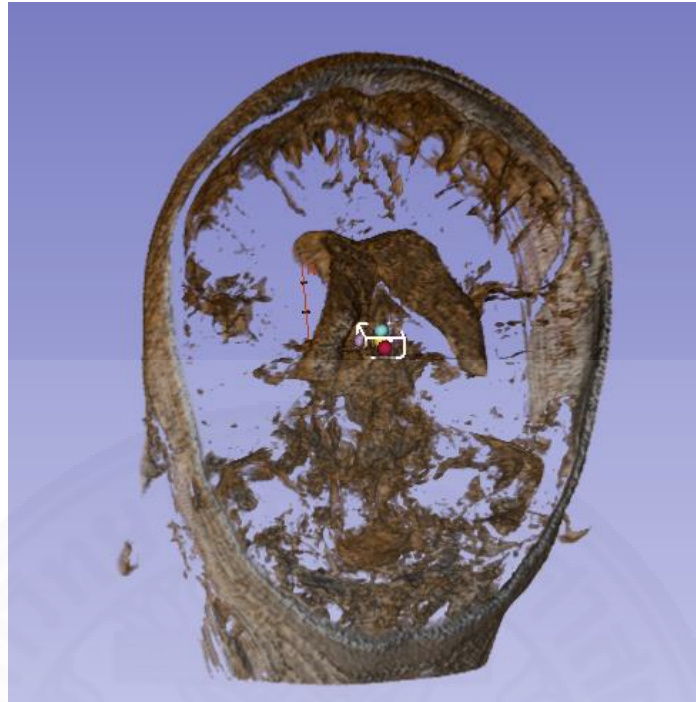
Figure 4.6. Region of interest (ROI)-Place of cerebral aqueduct

Region of interest (ROI)-Place of cerebral aqueduct is shown in Figure 4.6.

4.1.2 Solid models of Aqueduct of Sylvia

Solid models were built by using SOLIDWORKS PREMIUM 2015. Length of the aqueduct for both cases was considered as 14.1 mm and narrowest point was placed 8.5 mm distance from 3rd ventricle side of the solid model.

(a)
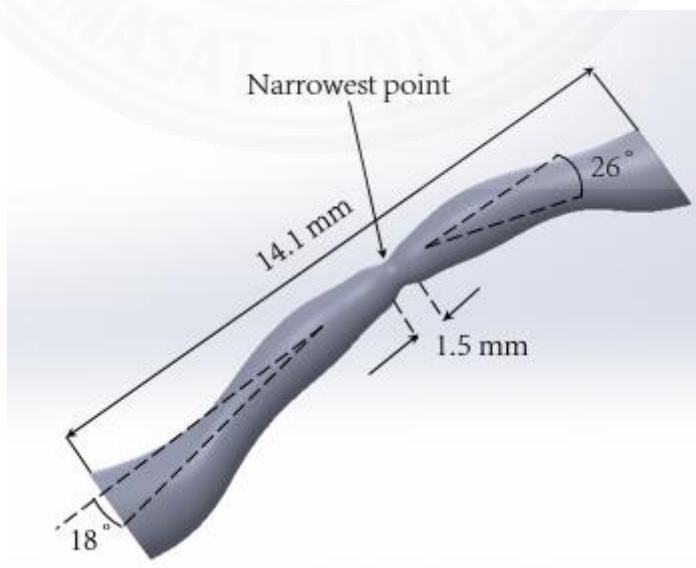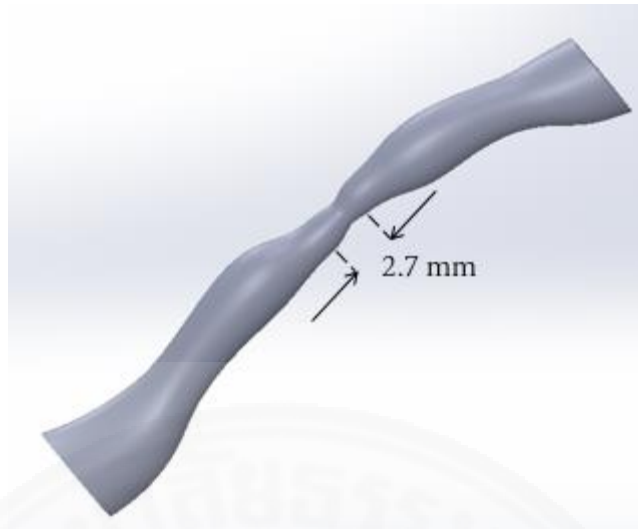
Figure 4.7. (a) and (b) shows Solid models of cerebral aqueduct for normal patient
and Normal pressure Hydrocephalus patient

Length of the narrowest point of normal patient's aqueduct was 1.5 mm
and 2.7 mm for NPH patient in axial direction of aqueduct. Diameter of the narrowest
point of aqueduct has been considered as 0.9 mm and 0.6 mm for normal patient and
NPH patient correspondingly. Figure 4.7 (a) and (b) shows the solid models of
aqueduct of Sylvia for normal patient and NPH patient correspondingly.

4.1.3 CFX Transient analysis for CSF flow through aqueduct

Solid models were imported to the ANSYS$^{©}$ and meshed as advanced size
function meshing on curvature surfaces. For both analysis, CSF has concerned as
water and aqueduct wall has concerned as solid material. Elasticity of the aqueduct
wall has changed to high and low for normal patient and Normal Pressure
Hydrocephalus patient respectively (Simulations has done by considering same wall
elasticity for normal and NPH case, there were not significant velocity distribution
change due to the compensation of pressure by elastin the wall of narrow point in
aqueduct). Initial boundary conditions were concerned as same for both analysis,
reference pressure of 3rd ventricle as 10mmHg. Velocity profile derived from
retrospective numerical analysis has been used as a mathematical expression to both
cases and initial CSF input velocity in to aqueduct from 3rd ventricle was set as

defined expression. Defined mathematical expression in CFX was for a one cycle of CSF pulsatile velocity.

For both analysis, CSF concerned as water and aqueduct wall concerned as solid elastic material by assigning brain tissue elastic properties. Elasticity of the aqueduct wall changed to 6000 Pa and 1500 Pa (Soza, et al., 2005) for normal patient and NPH patient respectively (Simulations has done by considering same wall elasticity for normal and NPH cases, there were no significant velocity distribution change due to the compensation of pressure by elastic property of the wall of aqueduct's narrow point). Initial boundary conditions were concerned as the same for both analysis, reference pressure of 3rd ventricle as 10 mmHg. Velocity profile derived from retrospective numerical analysis were used as a mathematical expression to both cases and initial CSF input velocity in to aqueduct from 3rd ventricle was set as defined expression (defined equation for CSF velocity profile was in our previous studies). Defined mathematical expression in CFX was for a one cycle of CSF pulsatile velocity. In order to get more accurate results, considered pulsatile cycle were divided in to 16 time steps.
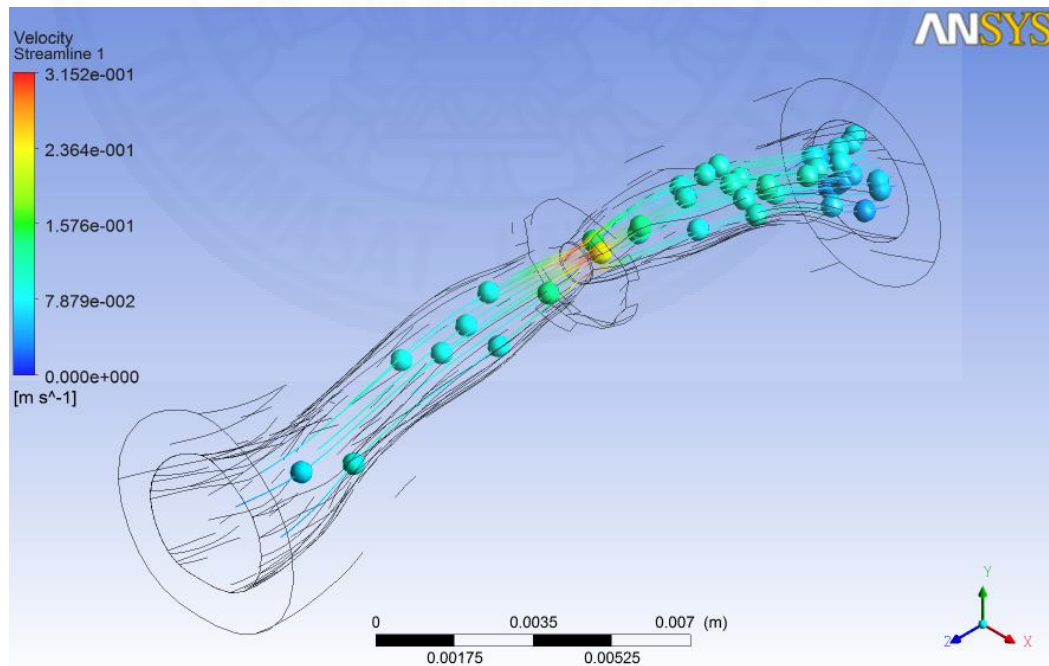
Figure 4.8. CSF velocity distribution through the aqueduct of normal patient

45

For a normal patient, maximum CSF velocity reached to 31.5 cm/s at narrowest point as shown in Figure 4.8. But for a Normal Pressure Hydrocephalus patient it reached to 51.7 cm/s as shown in Figure 4.9.
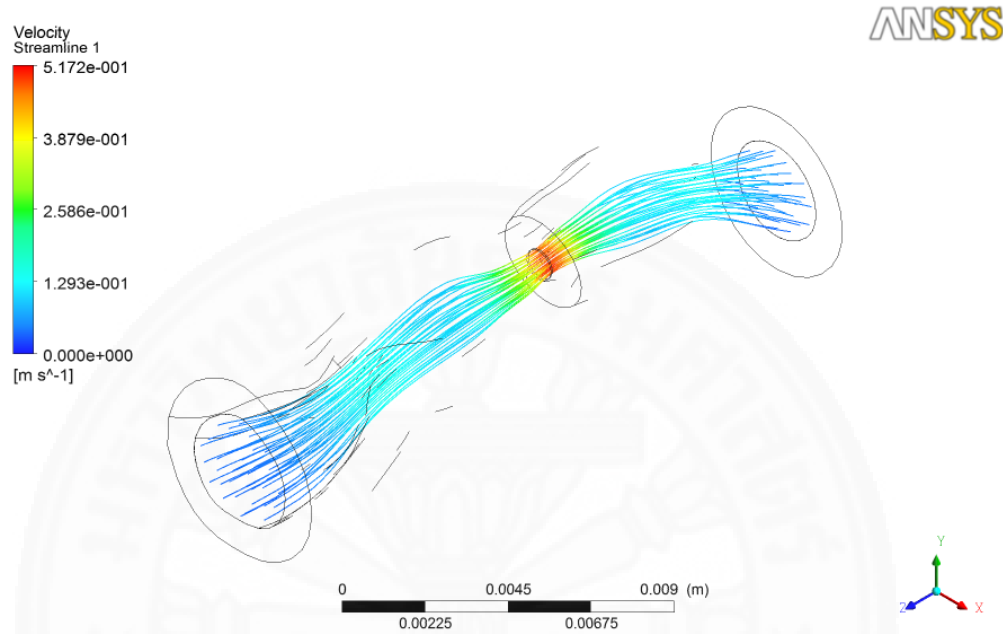
Figure 4.9. CSF velocity distribution through the aqueduct of Normal Pressure Hydrocephalus patient

According to the Venturi effect, lowest pressure exerted on the place of maximum velocity occurred. In contrast ascending velocity gradient exist along the third ventricle direction.

Navier-Stokes equation for motion of CSF can be written as refer to "(4.1)". Where u is fluid velocity, R_e is Reynolds number, f is force, and p is the mean of the three normal stresses.

$$\frac{Du}{Dt} = -\nabla p + f + \frac{1}{R_e}\nabla^2 u \qquad (4.1)$$

$$R_e = \frac{UL}{v}$$

Venturi effect can be illustrated as refer to "(4.2)".

$$P_{Third\ Ventricle} - P_{Narrowest\ Place} = \frac{\rho}{2}\left(v^2_2 - v^2_1\right) \qquad (4.2)$$

Where v_1 is the CSF velocity, at 3rd ventricle side and v_2 is the CSF velocity at narrowest point of aqueduct.

If the aqueduct wall elasticity is not enough to compensate the pressure increment, 3rd ventricle will enlarge as a consequence. With that results, we can conclude that ventricular enlargements can exert due to the reduction of cross sectional area at narrow point of aqueduct and the wall elasticity of narrow point. CFD results showed that, maximum CSF velocity of normal patient reached to 31.5 cm/s at narrowest point of aqueduct as shown in Figure 4.10. But for a NPH patient it reached to 51.7 cm/s as shown in Figure 4.11.

After that, velocity variation of CSF through the narrowest point of aqueduct for one R-R cycle has been plotted by based on the same input conditions on CFD analysis. Fig. 6(a) and Fig. 6(b) shows the CSF velocity profile at narrowest point of aqueduct of Sylvia for a one R-R cardiac cycle of normal patient and NPH patient correspondingly.
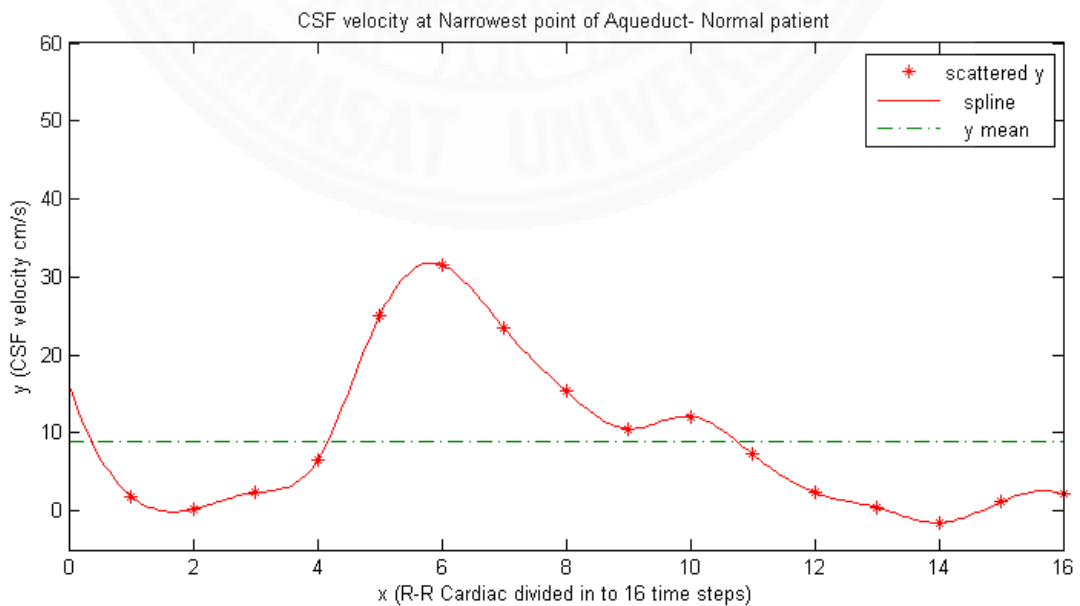
Figure 4.10. CSF velocity variation through the narrowest point of aqueduct of Sylvia for normal patient

47

Results implied that, CSF mean velocity of NPH patient at the narrowest point of aqueduct is higher than the cerebral spinal fluid mean velocity of normal patient at the narrowest point of aqueduct. Amplitude of peak velocity of CSF for NPH patient was significantly higher than the amplitude of peak velocity of CSF for normal patient.
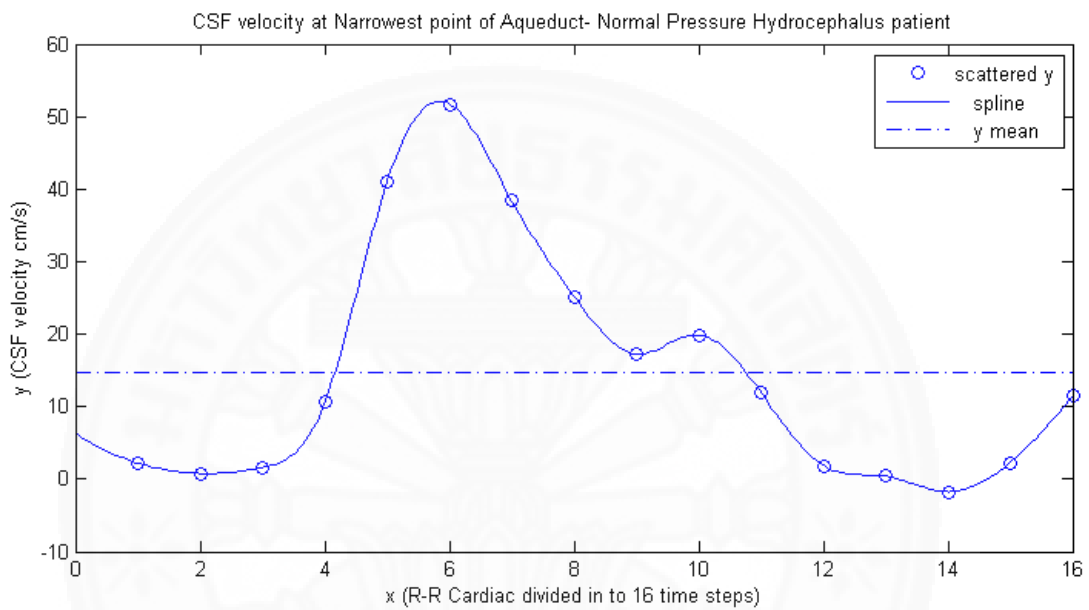
Figure 4.11. CSF velocity variation through the narrowest point of aqueduct of Sylvia for NPH patient

According to the Venturi effect, lowest pressure exerted on the place of maximum velocity occurred at a tube of fluid flows. Same phenomena happen in the aqueduct of Sylvia and lowest CSF pressure exists on the narrowest point. In contrast descending velocity gradient exists along the third ventricle direction and ascending pressure gradient exists in third ventricle direction from narrowest point of aqueduct. Investigations of Jeong Hyun Lee et al. (Lee, et al., 2004) have noted that same result as CSF velocity tendency to increase its velocity from the superior to the inferior aqueduct. At the narrowest point of the aqueduct, CSF pressure of NPH patient is lower than CSF pressure of normal patient. But, pressure gradient of NPH patient along the 3rd ventricle side is higher than the pressure gradient of normal patient along the 3rd ventricle side. If the aqueduct wall elasticity is significantly low and could not compensate the pressure increment, 3rd ventricle will enlarge as a consequence.

48

According to the results, we can conclude that ventricular enlargements might result from the reduction of cross sectional area or obstruction at narrow point of aqueduct and also the reduction of wall elastic property at narrowest point.

4.1.4 Intracranial Pressure and ventricular expansion

Cerebrospinal fluid pressure, defined as the intracranial pressure in the prone position, is the result of a dynamic equilibrium between CSF secretion, absorption and resistance to flow. CSF pressure can be measured invasively by a pressure transducer placed in the brain parenchyma or connected to CSF spaces via an external lumbar drain or external ventricular drain. Non-invasive methods essentially consist of interpretation of vascular flow on Doppler ultrasound. A method currently under investigation records the electrophysiological activity of outer hair cells of the cochlea. CSF pressure transmitted via the cochlear aqueduct influences intralabyrinthine pressure and the electrophysiological activity of outer hair cells. Monitoring of outer hair cell activity can therefore be used to monitor intracranial pressure variations (Büki, de Kleine, Wit, & Avan, 2002), (Chomicki, et al., 2007), (Traboulsi & Avan, 2007).

Since CSF space is a dynamic pressure system, CSF pressure determines intracranial pressure with physiological values ranging between 3 and 4 mmHg before the age of one year, and between 10 and 15 mmHg in adults. Apart from its function of hydromechanical protection of the central nervous system, CSF also plays a prominent role in brain development and regulation of brain interstitial fluid homeostasis, which influences neuronal functioning (Sakka, Coll, & Chazal, 2011). Any malfunctioning in CSF formation and motion cause to the expansion of ventricular system.

In contrast, we have done a Statistic pressure analysis of CSF in ventricular system for both normal and normal pressure hydrocephalus patient to understand the respond of ventricular system against varies morpometric conditions of aqueduct of Sylvia. Analysis was done for a 2D ventricular system by considering aforementioned morphometrics of aqueduct and buffering effect of ventricular system by assigning elastic properties to the ventricular wall. Modeling detail ascribed to the simulation is elsewhere to other studies which has been done by researchers.

49

Considered CSF pressure for normal and normal pressure hydrocephalus were 12mmHg and 20 mmHg respectively. Elasticity of the ventricular wall was considered as 6000 Pa.
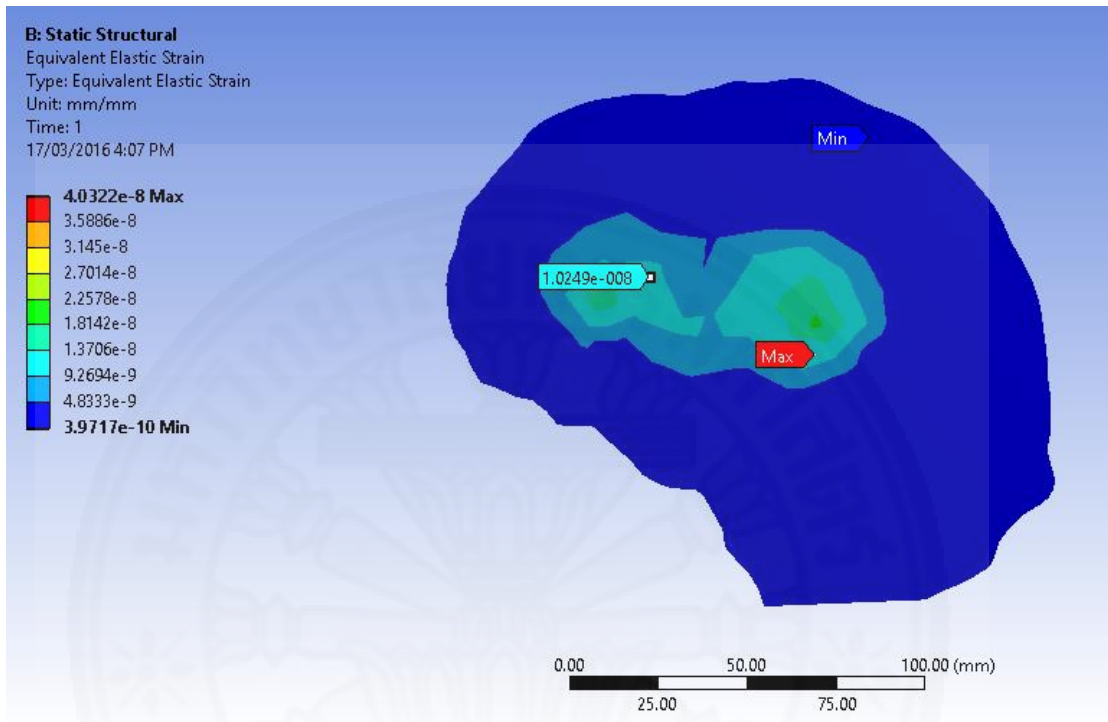
Figure 4.12. Strain of aqueduct and ventricular wall of normal patient under the 12mmHg CSF pressure

Results shows that highest strain of ventricle occurred at the pre-aqueduct of Sylvia while lowest strain occurred at the front horn of the lateral ventricles as illustrated in Figure 4.12. Results implied that, aqueduct wall expand to regulate the pressure inside the ventricles when it start to get increased.

Figure 4.13 shows the strains of ventricular system of NPH patient under the 10mmHg CSF pressure. Results implied that highest strain occurred in frontal part of lateral ventricles instead regulating CSF pressure by adjusting the size of aqueduct while strain of aqueduct showing the significantly low strain value.
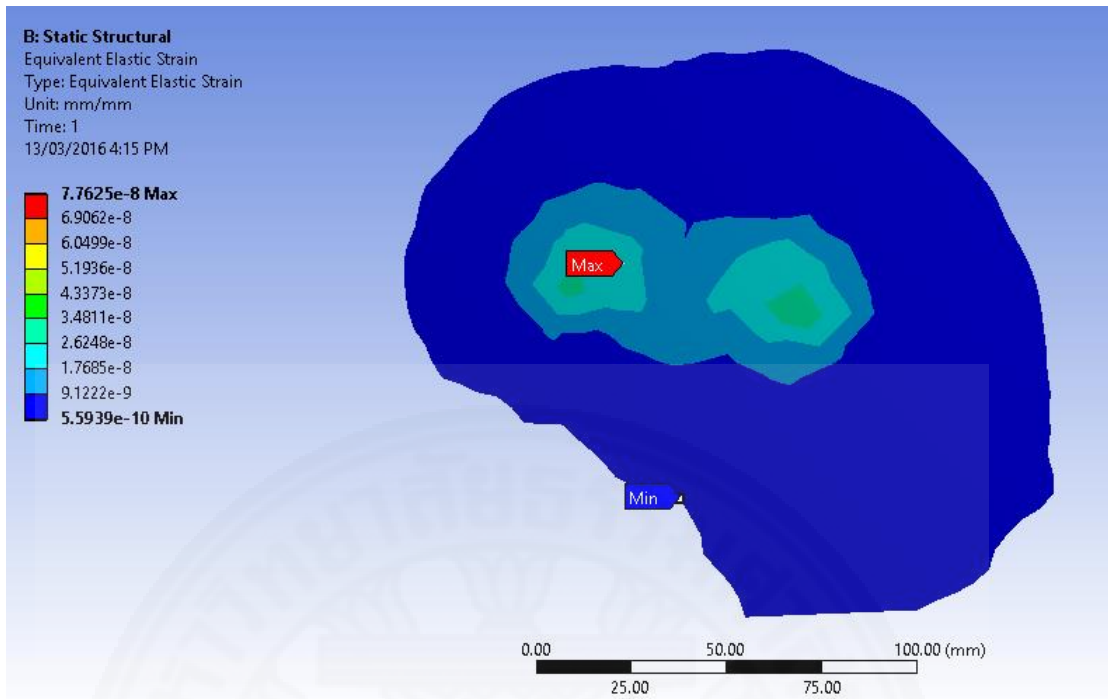
Figure 4.13. Strain of aqueduct and ventricular wall of normal pressure hydrocephalus patient under the 20mmHg CSF pressure

Results inferred, obstruction in aqueduct due to the morphometric irregularities leads to the ventricular expansion as a consequence of CSF pressure generates in ventricular system.

The CSF outflow from the cranial cavity to subarachnoid space is impacted by geometry of the aqueduct and CSF flow behavior through the aqueduct reflects the Intraventricular pressure and prognosticate the ventricular expansion. For a healthy person, brain expansion is typically very small and occurs simultaneously with an inflow of CSF (Greitz, Cerebrospinal fluid circulation and associated intracranial dynamics. A radiologic investigation using MR imaging and radionu clide cisternography, 1993). As shown in Figure 4.12, the highest ventricular expansion occurs in pre aqueduct while lowest ventricular expansion appears in lateral ventricle horn. Results interpreted that, for a normal patient, intraventricular pressure regulation cause by expanding the aqueduct and it helps to increase the CSF outflow from 3rd ventricle to 4th ventricle rather not trapping inside the lateral ventricles. But for a Normal pressure hydrocephalus condition, maximum ventricular expansion appears at frontal horn of lateral ventricle while the minimum expansion reported in pre

aqueduct as shown in Figure 4.13. Results implies, lateral ventricle expansion occur rather than regulating the intraventricular pressure regulation.

Similar research has been done by Brian J. Sweetman (Sweetman B. J., 2011) for his PhD research and found qualitative differences in the CSF flow patterns between the normal and hydrocephalic case as displayed in Figure 4.14. At mid systole, the pontine CSF flow is larger in the normal case, but the aqueductal CSF flow is larger in the hydrocephalic case. In normal subjects, the flow velocity amplitude is much higher in the prepontine area than in the aqueduct. In hydrocephalus, the aqueduct flow is increased, while the velocity in the prepontine area is reduced. The ratio of the aqueduct to the prepontine velocity amplitude is about seven times larger in hydrocephalic cases than in normals. This change suggests that the ratio of the prepontine to the aqueduct flow amplitude could be an indicator for the status of communicating hydrocephalus. While this ratio has not been used for diagnosis yet, its significance might be confirmed in future research.
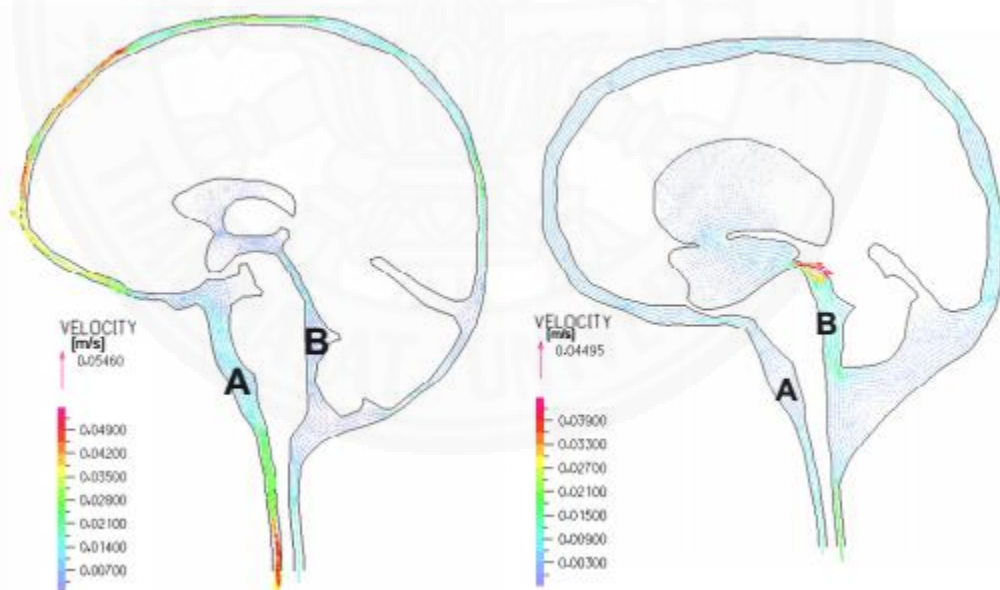
Figure 4.14. Simulated CSF flow pattern changes in the pontine cistern (A) and aqueduct (B) for normal (left) and hydrocephalic (right) subjects. CSF pontine flow is more pronounced in the normal case, whereas CSF flow is higher in the aqueduct and ventricular pathways under hydrocephalic conditions (Sweetman B. J., 2011)

The force responsible for ventricular enlargement in hydrocephalus is the intraventricular pressure pulse from accumulated CSF inside the ventricles (Wilson &

Bertan, 1967). For an intact skull, volume of brain, blood and CSF is constant. Enlargement in any of these factor will cause decrease in one or two of other components. This relationship provides a compensatory aspect to prevent the head in series damage with respect to ventricular expansion. Expansion of ventricles cause higher pressure in the cortex from it being pushed into the skull. Interplay between the demands for space by those three components of the intracranial content cause to increase in Intracranial pressure (ICP). In normal condition, increasing CSF absorption or reduction of rate of CSF manufacturing happen to compensate the space demand. Nevertheless, in Normal pressure hydrocephalus, these aspects are not further executed due to the exceeding of threshold limit by resulting CSF accumulation inside the ventricles. ICP is the result of a dynamic equilibrium between CSF secretion, absorption and resistance to flow. Higher elevation resistance to flow of CSF correspond to intracranial hypertension with irreversible brain damage (Sakka, Coll, & Chazal, 2011), (Büki, de Kleine, Wit, & Avan, 2002), (Chomicki, et al., 2007), (Traboulsi & Avan, 2007). ICP pressure above the 5-10 mmHg considered as elevated pressure.

Normal pressure hydrocephalus can grow to Hydrocephalus state. When ventricle expand, lateral ventricles and medial parts of the temporal lobes expand and compress the aqueduct. As a result, the pressure within the fourth ventricle drops and causes the aqueduct to close more tightly (Fin & Grebe, 2003), (Balédent, Henry-Feugeas, & Idy-Peretti, 2001).

4.2 Discussion

Theoretical and clinical experimental studies have been able to demonstrate some phenomenal circumstance of CSF formation and its effects on hydrocephalus. But, exact root causes are still controversy and yet to be identified. In this hypothetical study, objective was being to definite the theoretical framework that embodies in,

- The nature of the CSF-circulation, e.g., the magnitude and pattern of pulsatile and bulk flow

- The driving forces of the CSF circulation and assessment of the role of associated hemodynamics and brain motions
- Demonstrating that the effects of aqueductal morphometries in ventricular expansion

The derived mathematical model shows a pulsatile motion of CSF synchronizing with arterial pulsation. Maximum velocity of CSF has been derived as 2.275 cm/s by math model.

CSF motion is a combined effect of CSF production rate and cardiac pulsations. CSF production rate from its sites give a driving force to CSF while dominant power is being given by arterial dialation and contraction cause due to the cardiac pulsation. Arterial wall expand and contract during the systole and diastole respectively. Mechanical energy of arterial wall expansion and contraction transforms to the ventricular tissues which are contacting each other. Since both arterial walls and ventricular tissues constitute by endothelium cells, mechanical force transmission can be attributed to the spring system which are connected in series. Transmitted mechanical force to the ventricles govern the CSF to its sites of Sub arachnoid spaces via CSF pathway as shows in Figure 2.1.

T2 weighted 3T MRI images were taken from three control subjects to reconstruct the 3D models of ventricular system. Two patients were subjects were normal healthy and one patient was Normal Pressure Hydrocephalus. Geometric information ware taken from three dimensionally re-constructed models and solid models built based on that information. Velocity variation and magnitudes of CSF for both normal and NPH patient were quantified by CFD analysis and CSF velocity of NPH patient at narrowest point of aqueduct was significantly higher than the CSF velocity of normal patient at narrowest point of the aqueduct. CSF velocity of NPH patient at narrowest point counted as almost 10 time higher than its normal speed while Brian J. Sweetman (Sweetman B. J., 2011) noticed it as 7 time higher than normal speed of CSF.

Further, CFD results shows a significant relationship in magnitude of the CSF velocities of normal and NPH patients.
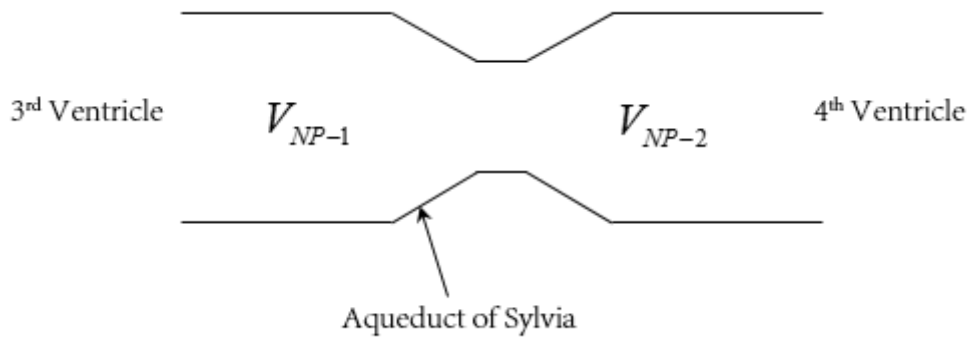
Figure 4.15. CSF velocity representation of aqueductal diarch for normal patient
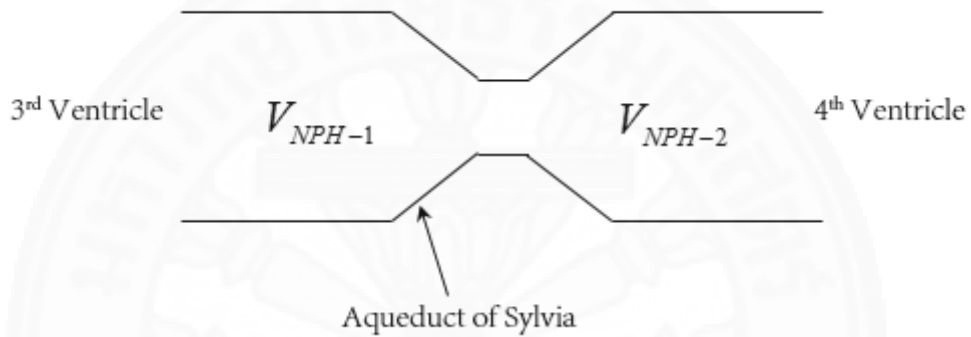
Figure 4.16. CSF velocity representation of aqueductal diarch for NPH patient

Compared in detail are the CSF flows in two regions of interest - in the aqueduct of Sylvius of 3rd ventricle side and 4th ventricle side as shown in Figure 4.15 and Figure 4.16. In normal subjects, average CSF flow velocity at 3rd ventricle side is more or less 3.5 cm/s and more or less 3.3cm/s at 4th ventricle side. In normal pressure hydrocephalus, CSF velocity near to 3rd ventricle out is more or less 2.8cm/s and 2.4cm/s near to 4th ventricle inlet. This change suggests that the ratio of the CSF velocity at 3rd ventricle outlet and 4th ventricle inlet is an indicator for the status of normal pressure hydrocephalus.

$$V_{NP\text{-}1} \qquad = \qquad 3.5 \pm 0.5 \text{ cm/s}$$

$$V_{NP\text{-}2} \qquad = \qquad 3.5 \pm 0.3 \text{ cm/s}$$

$$V_{NPH\text{-}1} \qquad = \qquad 2.5 \pm 0.5 \text{ cm/s}$$

$$V_{NPH\text{-}2} \qquad = \qquad 2.5 \pm 0.1 \text{ cm/s}$$

$$V_{NP\text{-}1} - V_{NP\text{-}2} \qquad = \qquad \Delta_{NP}$$

$$V_{NPH\text{-}1} - V_{NPH\text{-}2} \qquad = \qquad \Delta_{NPH}$$

$$\Delta_{NPH} \qquad > \qquad \Delta_{NP}$$

While this ratio has not been used for diagnosis yet, its significance might be confirmed in future research. For Hydrocephalus patients, CSF velocity has been noted as, very low value at the 4th ventricle inlet (Sweetman B. J., 2011).

Apart to the CSF velocity, analyzing the ventricular behavior with respect to the Intercranial pressure and aqueduct with different morphometrics also important to diagnose the hydrocephalus. Whereas, author has been done a 2D static structural simulation for the ventricular system under the 6mmHg and 10mmHg intercranial pressure corresponding to normal and NPH patient. Elastic wall properties has been assigned to the ventricular and aqueduct wall. Aqueduct was designed by considering realistic morphometric values as measured. Results implied that, there is a tendency to expand the lateral ventricles of NPH patient and expansion of aqueduct to regulate the intercranial pressure of normal patient.

4.2.1 Intracranial pressure elivation

Intracranial pressure elevation is a severe problem encountered in neurological and neurological practices. It can be caused as an impact of mass lesion, malfunctions in CSF motion or passive conditions in intracranial biological processes. As hypothesis stated by Monro-Kellie, volume and pressure inside the cranium shows a non-linear relationship verses each other as shows in Figure 4.17. Since skull is fixed volume rigid object which is occupied by cerebral blood, CSF and brain, increase in any of these component must be offset by decreasing one or more of the other components to compensate the volume demand. This biological phenomena helps to regulate the ICP of normal healthy people without allowing ICP to surpass the threshold level. Cerebral blood and CSF are the most flexible components which can adapt easily to accommodate demand by brain. If one of these is malfunctioning, further increase of brain results an intracranial pressure elevation (Healthcare, 2003), (Avezaat, Eijndhoven, & Wyper, 1979).

56
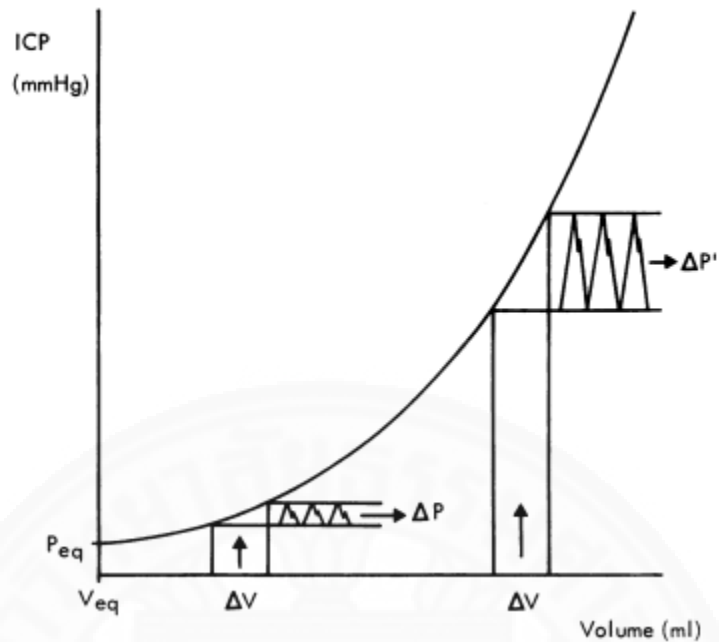
Figure 4.17. The CSF pulse pressure is a pressure response (ΔP) to the transient increase in intracranial blood volume during a cardiac cycle (ΔV). The exponential shape of the intracranial volume-pressure curve explains why the CSF pulse pressure increases with rising intracranial pressure (ICP) (Avezaat, Eijndhoven, & Wyper, 1979)

       The first of the curve illustrate the limited increase in pressure due to the compensatory reserve being large enough to accommodate the extra volume. With increasing volume, the compensatory reserve is eventually exceeded, using a rapid change in pressure. Obstructions in aqueduct leads to CSF accumulation in ventricles and ultimately increase in intracranial pressure.

Chapter 5

Conclusions and Recommendations

5.1 Research conclusion

Studies of CSF and ventricular system moves to centuries back from present. But, during past resent decade, these studies have been showing a new countenance resulting an extensive finding on ventricular system and CSF hemodynamics. Researchers and scientists tended to persevere researches on certain discretize parts on ventricular system and how those particular parts effects to the disorders associated with ventricular system. The aqueduct of Sylvius (AqSylv) likely becomes an increasing region of importance among researchers. However, currently there is no clear and adequate description on influence of aqueduct in disorders like hydrocephalus or its varieties like NPH or Communication hydrocephalus (Giesel, et al., 3D Reconstructions of the Cerebral Ventricles and Volume Quantification in Children with Brain Malformations, 2009). Pathophysiologically, hydrocephalus interpreted as imbalance of CSF formation and absorption. As described in the introduction chapter, CSF secrets from ventricular cavities and moves to absorption sites of subarachnoid spaces through the aqueduct passage. Malabsorption can be caused due to passive condition of arachnoid villi.

The theory that the root cause of Normal pressure hydrocephalus (NPH) is an abnormal accumulation of cerebrospinal fluid (CSF) in the ventricular cavities. But the phenomena of how it caused is not circumstantiated by either experimental or by clinical evidence. Any age of individual can be subjected to Normal pressure hydrocephalus, but clinical records shows that is positively common in adults. Medical doctors and researchers have been counting it may result from a head trauma, mass lesion, infection or subarachnoid hemorrhage. Nevertheless, many NPH patients have been reported without presence of any aforementioned factors. Then, root cause of particular disorder considered as unknown.

Generally, laboratory testing and imaging studies like MRI and CT are not applicable (Still MRI is better than CT scanning in diagnosis of NPH) in diagnosis of normal pressure hydrocephalus (Schneck, n.d.). Conventional diagnosis of the NPH

done based on the symptoms of the patient such like, abnormal gait, Urinary incontinence and Dementia. Gait disturbance is the most common and prioritized aspect to noted and considered to be the most responsive to treatments. According to the findings of Sakakibara et.al. (Sakakibara, et al., 2008) urinary symptoms are, frequency of urinary release requirement, urgency and or frank incontinence. On their study, 95% of patients had urodynamic parameters consistent with detrusor overactivity. From the observations of Bech-Azeddine et.al, they noticed higher value than 60% of NPH subjects they observed had cardiovascular disease (Bech-Azeddine, Hogh, Juhler, Gjerris, & Waldemar, 2007). Further, in another similar study, more than 75% had Alzheimer disease pathology at the time of shunt surgery (Golomb, et al., 2000).

After referring physical observation and previous clinical records, patient is recommended to attend for further testing. Patients which is showing a gradually progressive disorder is suspected as NPH, and should receive shunt treatment like lumber puncture or lumber drainage. CSF amount need to be removed is a perception for NPH (Aimard, Vighetto, Gabet, Bret, & Henry, 1990).

In this study, we convincingly proved that, normal pressure hydrocephalus can be caused due to obstruction in aqueduct, and geometrical shape of aqueduct significantly influenced to state of Normal pressure hydrocephalus elsewhere the malabsorption of CSF. Additionally, we attested how geometry of aqueduct effects to ventricular expansion and co-relation of CSF velocity variation to normal pressure hydrocephalus diagnosis.

In contrast, since imaging tests and laboratory testing are not viable enough to recognize the NPH, we developed a correlation to diagnosis NPH elsewhere the traditional methods via conducting comprehensive analysis and simulations. Referred to the results, we found that, Normal pressure hydrocephalus can be caused due to an obstruction for CSF flow through the aqueduct ascribe to abnormalities or blocked in some way. Ultimately leads to the ventricular expansion resulting the intracranial pressure. It implies that, term of "normal pressure" is somewhat controversy. Since, Normal pressure hydrocephalus (NPH) is a sub-category of hydrocephalus, this study could be helpful to improvements in diagnosis

of NPH and Hydrocephalus. As a synopsis of the research, we have addressed to the below facts,

- The nature of the CSF-circulation, e.g., the magnitude and pattern of CSF flow: CSF has a pulsatile motion synchronized with the arterial pulsation.
- The governing forces of the CSF circulation: Governing force of CSF motion is a combined effect of CSF formation rate and cardiac pulsations. Systolic expansion and diastolic contraction of intracranial arteries transmit energy to CSF via the intraventricular tissues engaged with arterial blood walls. CSF dominantly driven by arterial daialtion and contraction effect.
- CSF velocity of NPH patient at narrowest point of aqueduct is significantly higher than the CSF velocity of normal patient at the narrowest point of aqueduct.
- Influence of Aqueduct geometry to ventricular expansion.
- The ratio of the CSF velocity at 3rd ventricle outlet and 4th ventricle inlet is an indicator for the status of normal pressure hydrocephalus.
- Shape of the aqueduct also affect to the obstruction hydrocephalus.
- In NPH patients, lateral ventricle start to expand by responding to the increased Inter-ventricle pressure while aqueduct of Sylvia regulate the Inter-ventricle pressure of normal patients by expanding the cross section area of aqueduct.

Diagnosis of normal pressure hydrocephalus is one of the difficult clinical problems, not only because of overlapping with other syndromes but also because of the heterogeneity of the treatment response that influences the study designs. Studies of CSF flow analysis by using normal subjects were not successful because when hydrocephalus had developed, the dilated aqueduct resulted in change of area and volume was author's region of interest (ROI).

A number of roles have been attributed to cerebrospinal fluid (CSF) over the years, ranging from that of a static mechanical brain protection medium, to a steadily flowing metabolite collector and to a neuroendocrine communication pathway. Now, there is a growing body of evidence suggesting that CSF also plays an

important role in the development and organization of the central nervous system through neuronal guidance.

5.2 Recommendation for future works

As an extension of this research work, I would like to recommend a research topic on designing a stent to deduct the restriction of narrowest point of aqueduct by enlarging the particular stenosis place. Further, analysis of compressible stresses that stent can beard and its deformable ability with respect to the applied forces on it could be important. MATLAB Simulink could use to define the aqueduct wall environment including its spring ability, stiffness and forces undergoes. Figure 5.1 shows a stent placed in an arterial as an example for stent.
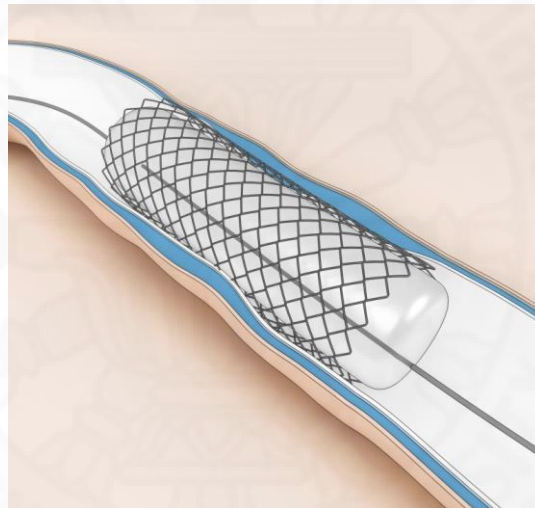
Figure 5.1. Prosthesis stent as a solution for stenosis in blood artery (Beam, 2016)

Computational fluid dynamics analysis for stent implanted aqueduct would help to identify the respond of stent with respect to the sinusoidal motion of CSF along the aqueduct.

References

Africa, r. (n.d.). *Hydrocephalus*. Retrieved from BookMed: http://book-med.info/hydrocephalus/10654

Aimard, G., Vighetto, A., Gabet, J., Bret, P., & Henry, E. (1990). Acetazolamide: an alternative to shunting in normal pressure hydrocephalus? Preliminary results. *Rev Neurol (Paris), 146*(6-7), 437-439.

Ambarki, K., Baledent, O., Kongolo, G., Bouzerar, R., Fall, S., & Meyer. (2007, March). A New Lumped-Parameter Model of Cerebrospinal Hydrodynamics During the Cardiac Cycle in Healthy Volunteers. *IEEE Transaction on Biomedical Engineering, 54*(3), 483-491.

Anthony M, A. M., & Benjamin S, C. S. (2009). *Increased intracranial pressure. Current Management in child Neurology* (Vol. Third edition). BC Decker Inc.

Anthony, M. P., Kenneth, S. M., & Roberto, M. R. (1978). A Nonlinear analysis of the cerebrospinal fluid system and intracranial pressure dynamics. *J Neurosurg, 48*, 332-344.

Avezaat, C. J., Eijndhoven, J. H., & Wyper, D. J. (1979, August). Cerebrospinal fluid pulse pressure and intracranial volume-pressure relationships. *J Neurol Neurosurg Psychiatry, 42*(8), 687-700.

Balédent, O., Henry-Feugeas, M., & Idy-Peretti, I. (2001, July). Cerebrospinal fluid dynamics and relation with blood flow: a magnetic resonance study with semiautomated cerebrospinal fluid segmentation. *Invest Radiol, 36*(7), 368-377. doi:PMID: 11496092

Beam, J. (2016, June). *What is a Stent*. (N. Foster, Editor) Retrieved from wiseGEEK: http://www.wisegeek.com/what-is-a-stent.htm

Bech-Azeddine, R., Hogh, P., Juhler, M., Gjerris, F., & Waldemar, G. (2007, February). Idiopathic normalpressure hydrocephalus: clinical comorbidity correlated with cerebral biopsy findings and outcome of cerebrospinal fluid shunting. *J Neurol Neurosurg Psychiatry, 78*(2), 157-161.

Boston Children's Hospital, H. (n.d.). *Thriving*. Retrieved from Boston Children's Hospital's pediatric health blog: http://thriving.childrenshospital.org/childrens-doctor-imporves-hydrocephalus-treatment-in-africa/

Bradley Jr, W. (2015, May). CSF Flow in the Brain in the Context of Normal Pressure Hydrocephalus. *AJNR Am J Neuroradiol , 36*(2), 831–838.

Brook, B., Falle, S., & Pedley, T. (1999). Numerical solutions for unsteady gravity driven flows in collapsible tubes: evolution and roll wave instability of a steady state. *Journal of Fluid Mechanics, 396*, 223-256.

Büki, B., de Kleine, E., Wit, H., & Avan, P. (2002, May). Detection of intracochlear and intracranial pressure changes with otoacoustic emissions: a gerbil model. *Hear Res, 167*(2), 180-191.

Chomicki, A., Sakka, L., Avan, P., Khalil, T., Lemaire, J., & Chazal, J. (2007, August). Derivation of cerebrospinal fluid: consequences on inner ear biomechanics in adult patients with chronic hydrocephalus. *Neurochirurgie, 53*(4), 265-271.

Dunn, L. T. (2002). RAISED INTRACRANIAL PRESSURE. *J Neurol Neurosurg Psychiatry, 73*, 23-27.

Egnor, M., Zheng, L., Rosiello, A., Gutman, F., & Davis, R. (2002). A model of pulsations in communicating hydrocephalus. *Pediatr. Neurosurg, 36*(6), 281-303.

Enzmann, D. R., & Pelc, N. J. (1993, November). Cerebrospinal Fluid Flow Measured by Phase-Contrast Cine MR. *AJNR Am J Neuroradiol, 14*(6), 1301-7.

European, r. (n.d.). *Hydrocephalus*. Retrieved from Sabeel Homeo Clinic: http://www.sabeelhomeoclinic.com/perfect-homeopathic-treatment-of-hydrocephalus-babies-in-pakistan.html

Fin, L., & Grebe, R. (2003, June). Three dimensional modeling of the cerebrospinal fluid dynamics and brain interactions in the aqueduct of sylvius. *Computational Methods in Biomechanical and Biomedical Engineering, 6*(3), 163-170.

Furlan, J., Kadambi, J., Loparo, K., Sreenath, S., & Manjila, S. (2008, August 17-20). Investigation of CSF flow characteristics within a Rapid Prototype based model of the cerebral ventricular system using PIV. *The 19th International Symposium on Transport Phenomena*.

Giesel, F. L., Hart, A. R., Hahn, H. K., Emma, W., Fabian, R., Roland, T., . . . Griffiths, P. D. (2009, May). 3D Reconstructions of the Cerebral Ventricles and Volume Quantification in Children with Brain Malformations. *Academic Radiology, 16*(5), 610-617.

Giesel, F. L., Hart, A. R., Hahn, H. K., Wignall, E., Rengier, F., Talanow, R., . . . Griffiths, P. D. (2009, May). 3D Reconstructions of the Cerebral Ventricles and Volume Quantification in Children with Brain Malformations. *Academic Radiology, 16*(5), 610-617.

Golomb, J., Wisoff, J., Miller, D., Boksay, I., Kluger, A., Weiner, H., . . . Graves, W. (2000, June). Alzheimer's disease comorbidity in normal pressure hydrocephalus: prevalence and shunt response. *J Neurol Neurosurg Psychiatry, 68*(6), 778-781.

Greitz, D. (1993). Cerebrospinal fluid circulation and associated intracranial dynamics. A radiologic investigation using MR imaging and radionu clide cisternography. *Radiol Suppl, 386*, 1-23.

Greitz, D., Nordell, B., Ericsson, A., Sthlberg, F., & Thomsen, C. (n.d.). Notes on the driving forces of the CSF circulation with special emphasis on the piston action of the brain. *Proceedings of the XIV Symposium Neuroradiologicum, 33*, 178-181.

Hakim, S., & Adams, R. (1965, July). The special clinical problem of symptomatic hydrocephalus with normal cerebrospinal fluid pressure. Observations on cerebrospinal fluid hydrodynamics. *Neurological sciences, 2*(4), 307-327.

Hakim, S., Venegas, J., & Burton, J. (1976, March). The physics of the cranial cavity, hydrocephalus and normal pressure hydrocephalus: mechanical interpretation and mathematical model. *Surg Neurol,PubMed PMID:1257894, 5*(3), 187-210.

Haughton, V. M., Korosec, F. R., Medow, J. E., Dolar, M. T., & Iskandar, B. J. (2003, February). Peak Systolic and Diastolic CSF Velocity in the Foramen Magnum in Adult Patients with Chiari I Malformations and in Normal Control Participants. *AJNR Am J Neuroradiol, 24*, 169-176.

Healthcare, O. R. (2003). *Overview of Adult Intracranial Pressure (ICP) Management & Monitoring Systems.* Education & Development.

Hueng, C. F., Giiang, L.-H., Teng, Y. H., Juan, C.-J., Chen, C.-Y., Wang, A.-C., & Chen, S.-J. (2011). Cerebrospinal Fluid Flow Quantification of the Cerebral Aqueduct in Children and Adults with Two-Dimensional Cine Phase-Contrast Magnetic Resonance Imaging. *Fu-Jen Journal of Medicine, 9*(2).

Hydrocephalus, N. P. (2014). *Hydrocephalus.* Retrieved from Hydrocephalus association: http://www.hydroassoc.org/about-us/newsroom/facts-and-stats-2/

Lee, J. H., Lee, H. K., Kim, J. K., Kim, H. J., Park, J. K., & Choi, C. G. (2004, April). CSF Flow Quantification of the Cerebral Aqueduct in Normal Volunteers Using Phase Contrast Cine MR Imaging. *Korean J Radiol, 5*(2), 81-86.

Lindgren, E., & Di Chiro, G. (1953, February). The Roentgenologic Appearance of the Aqueduct of Sylvius. *Acta Radiol, 39*, 117-125.

Linninger, A. A., Tsakiris, C., Zhu, D. C., Xenos, M., Roycewicz, P., Danziger, Z., & Penn, R. (2005, April). Pulsatile Cerebrospinal Fluid Dynamics in the Human Brain. *IEEE Transactions on biomedical engineering, 52*(4), 71-79.

Linninger, A. A., Xenos, M., Zhu, D. C., Somayaji, M. R., Kondapalli, S., & Penn, R. D. (2007, February). Cerebrospinal Fluid Flow in the Normal and Hydrocephalic Human Brain. *IEEE Transactions on Biomedical engineering, 54*(2), 112-119.

Luetmer, P. H., Huston, J., Friedman, J. A., Dixon, G. R., Petersen, R. C., Jack, C. R., . . . Ebersold, M. J. (2002, March). Measurement of Cerebrospinal Fluid Flow at the Cerebral Aqueduct by Use of Phase-contrast Magnetic Resonance Imaging: Technique Validation and Utility in Diagnosing Idiopathic Normal Pressure Hydrocephalus. *Neurosurgery, 50*(3).

Marco, G. d., Peretti, I. I., Poncelet, A. D., Baledent, O., Onen, F., Cecile, M., & Henry, F. (2004, March). Intracranial Fluid Dynamics in Normal and Hydrocephalic States Systems Analysis With Phase-Contrast Magnetic Resonance Imaging. *J Comput Assist Tomogr, NEUROIMAGING, 28*(2), 247-254.

Masoumi, N., Bastani, D., Najarian, S., Ganji, F., Farmanzad, F., & Seddighi, A. S. (2010, Juny). Mathematical Modeling of CSF Pulsatile Hydrodynamics Based on Fluid Solid Interaction. *IEEE Transactions on Biomedical Engineering, 57*(6), 1255-63.

Matys, T., Horsburgh, A., Kirollos, R., & Massoud, T. (2013, December). The aqueduct of Sylvius: applied 3-T magnetic resonance imaging anatomy and morphometry with neuroendoscopic relevance. *Neurosurgery, 73*(2), 132-40. doi:10.1227/01.neu.0000430286.08552.ca

Mauro, U. (1988, July). A mathematical study of human intracranial hydrodynamics part 1—The cerebrospinal fluid pulse pressure. *Annals of Biomedical Engineering, 16*(4), 379-401.

Mauro, U. (1988). A mathematical study of human intracranial hydrodynamics part 2—Simulation of clinical tests. *Annals of Biomedical Engineering, 16*(4), 403-416.

McMillan, J., & Williams, B. (1977, June). Aqueduct stenosis. Case review and discussion. *J Neurol Neurosurg Psychiatry, 40*(6), 521–532.

Method, I. m. (n.d.). *Gaeltec news*. Retrieved from Gaeltec: http://www.gaeltec.com/news/article/10005/intracranial-pressure-monitoring/

Monro kellie, d. (n.d.). *Classconnection*. Retrieved from amazonaws: https://classconnection.s3.amazonaws.com/285/flashcards/674285/jpg/picture 51342119659286.jpg

Naidich, T., Altman, N., & Gonzalez-Arias, S. (1993, October). Phase contrast cine magnetic resonance imaging: normal cerebrospinal fluid oscillation and applications to hydrocephalus. *Neurosurg Clin N Am, 4*(4), 677-705.

National Institutes of Health, O. o. (n.d.). *Hydrocephalus Fact Sheet*. Retrieved from National Institute of Neurological Disorders and Stroke: http://www.ninds.nih.gov/disorders/hydrocephalus/detail_hydrocephalus.htm

Nervous System, D. (n.d.). *Aqueductal Stenosis*. Retrieved from http://www.nervous-system-diseases.com/aqueductal-stenosis.html

Neurosurgery, U. (n.d.). *Aqueductal Stenosis*. Retrieved from UCLA Health from: http://neurosurgery.ucla.edu/aqueductal-stenosis

Normal Pressure Hydrocephalus. (2013, August). Retrieved from Lifestyle: https://www.bostonglobe.com/2013/08/11/look-disorder/fL198IvjL2LT8uu0V1ePIK/story.html

Otto, F. (1899). Die grundform des arteriellen pulses. Erste Abhandlung, Mathematische analyse. *Z. Biol, 37*, 483-526.

Pathway, C. (n.d.). *CSF Pathway*. Retrieved from Wikipedia: https://en.wikipedia.org/wiki/Cerebrospinal fluid

Puncture, L. (n.d.). *Lumbar Puncture*. Retrieved from JuniorDentist: http://www.juniordentist.com/lumbar-puncture-needle.html

Reneman, R. S., Merode, T. V., Hick, P., Muytjens, A. M., & Hoeks, A. (1986, June). Age-related changes in carotid artery wall properties in men. *Ultrasound in Medicine & Biology, 12*(6), 465-71.

Sakakibara, R., Uchiyama, T., Kanda, T., Uchida, Y., Kishi, M., & Hattori, T. (2008, March). Urinary dysfunction in idiopathic normal pressure hydrocephalus. *Brain Nerve, 60*(3), 233-239.

Sakka, L., Coll, G., & Chazal, J. (2011, December). Anatomy and physiology of cerebrospinal fluid. *European Annals of Otorhinolaryngology, Head and Neck Diseases, 128*(6), 309–316. doi:10.1016/j.anorl.2011.03.002

Schneck, M. J. (n.d.). *Normal Pressure Hydrocephalus*. (S. R. Benbadis, Editor) Retrieved from MedScape: http://emedicine.medscape.com/article/1150924-overview

Simone, B., Dimos, P., & Vartan, K. (2012, June). Phantom model of physiologic intracranial pressure and cerebrospinal fluid dynamics. *IEEE Transaction on Biomedical Engineering, 59*(6), 1532-8.

Soza, G., Grosso, R., Nimsky, C., Hastreiter, P., Fahlbusch, R., & Greiner, G. (2005, Septeber). Determination of the elasticity parameters of brain tissue with combined simulation and registration. *Wiley InterScience, 1*(3), 87-95. doi:10.1581/mrcas.2005.010308

Spencer, M., & Dennison, A. (1963). Pulsatile blood flow in the vascular system. *In Handbook of Physiology, 2*(2), 839-864.

Spennato, P., Tazi, S., Bekaert, O., Cinalli, G., & Decq, P. (2013, February). Endoscopic Third Ventriculostomy for Idiopathic Aqueductal Stenosis. *World Neurosurgery, 79*, 1310-1320.

Sukhraaj, S. B., Harris, T. J., & Linninger, A. A. (2011, May). Dynamic Brain Phantom for Intracranial Volume Measurements. *IEEE Transaction on Biomedical Engineering, 58*(5), 1450-5.

Sweetman, B. J. (2011). *Cerebrospinal Fluid Flow in Normal and Hydrocephalic Brains.* Ph.D Thesis, University of Illinois at Chicago.

Sweetman, B., Xenos, M., Zitella, L., & Linninger, A. A. (2011). Three dimensional computational prediction of cerebrospinal fluid flow in the human brain. *Computers in Biology and Medicine, 41*(5), 67-75.

Thalakotunage, A., & Thunyaseth, S. (2015, January). Mathematical Model for Dynamics of CSF through the Aqueduct of Sylvia Based on an Analogy of Arterial Dilation and Contraction. *International journal of mining, metallurgy & mechanical engineering (IJMMME), 3*(4). doi:ISSN 23204060

Thunyaseth, S. (2013). *Mathematical Model for Hemodynamic and Intracranial Windkessel Mechanism.* Doctoral Thesis, Case Western Reserve University.

Traboulsi, R., & Avan, P. (2007, November). Transmission of infrasonic pressure waves from cerebrospinal to intralabyrinthine fluids through the human cochlear aqueduct: Non-invasive measurements with otoacoustic emissions. *Hear Res, 233*(1), 30-39.

Wilson, C., & Bertan, V. (1967, December). Interruption of the anterior choroidal artery in experimental hydrocephalus. *Arch Neurol, 17*(6), 614-619. doi:PMID: 6054895

Appendices

Appendix A

Nomenclature of equations

A_i	Cross section of the ventricular or sub-arachnoid section [m^2]
A_B	Projected cross section area of Arterioles inner wall [m^2]
$a(t)$	Choroid plexus displacement [m]
h_i	Height of the ventricular or subarachnoid section [m]
k_e	Brain tissue elasticity constant [N/m]
k_d	Brain tissue compliance [(N s)/m]
k_B	Spring constant of Arterioles [N/m]
F_i	Poiseuille Friction term [N/m^3]
F_B	Force exerted on internal wall of Arterioles [N]
l_i	Length of foramina connecting ventricles [m]
l_B	Length of Arterioles blood vessel [m]
$p_o(t)$	Pressure of brain parenchyma [N/m^2]
$p_i(t),p_{SAS}(t)$	CSF pressure in ventricles and subarachnoid section (ICP) [N/m^2]
$q_{e,j}(t)$	Reabsorption flow rate in a section [m^3/s]
$q_{f,i}(t)$	CSF production rate in the choroid plexus [m^3/s]
$q_i(t)=A_i v_i$	CSF flow rate leaving ventricle, i.e., flow in foramina and aqueduct [m^3/s]
r_i	Radius of the foramina and aqueduct [m]
r_B	Internal radius of Arterioles vessel [m]
$v_i(t)$	Axial CSF flow velocity [m/s]
$y_i(t)$	Tissue displacement in a section [mm]
$P_{Systolic}$	Systolic blood pressure [N/m^2]
$P_{Diastolic}$	Diastolic blood pressure [N/m^2]

Greek Symbols

δ_r	Arterioles wall displacement [m]
α	Amplitude of choroid expansion [m]
δ	Tissue width [m]
k	Reabsorption constant [m^3/(Pa s)]
μ	Fluid density [kg/m^3]

Appendix B
Simulink circuit diagram

Blood vessel simulink sumulation diagram